8

QUASI-THERMAL MODELS

Ramiro de la Reza

INTRODUCTION

The atmospheres of giant and supergiant stars of the M-, S-, C-type appear to be intrinsically very different from the late-type dwarfs. Although M dwarfs possess a chromosphere, a transition region, and a corona that are qualitatively similar to that of the Sun, these luminous giant and supergiant objects appear to be devoid of transition regions and coronae, but to be characterized by vast amounts of circumstellar matter (Rieu, Lefèvre, and Glassgold and Huggins, this volume) and often important mass loss (Goldberg, this volume). As shown by observations of highly ionized lines in the ultraviolet with the International Ultraviolet Explorer (IUE), there are no indications that plasmas of temperatures of 10^5 K, corresponding to a transition region, exist. A recent review on late-type IUE observations is given by Baliunas (1983). The same negative results were obtained by absence of direct detections of the X-ray fluxes by means of the Einstein Observatory Satellite, indicating the absence of coronae (Vaiana et al., 1981). Indirect observations of coronae made by observing the He I line at 10830 Å (Zirin, 1982) also gave negative results. This chromospheric line can be formed by a photoionization/recombination process, produced by illumination of a coronal radiation. Moreover, no lines from high stages of ionization were seen in a short wavelength exposure with IUE of the carbon star, TX Psc, with an exposure of 7 hours (Johnson and O'Brien, 1983).

Some recent evidences show that, above the photosphere, a vast chromosphere could exist (Stencel, 1982a), at least for the early red giants and supergiants, extending to several stellar radii. These chromospheres connect the photosphere to the circumstellar regions. The important mass loss observed in these stars begins to operate somewhere in these chromospheres. If these chromospheres are extended, a new problem appears: to find the mechanism that could support them—turbulence? magnetic field? The answers are not definite.

In our discussion and construction of quasi-thermal models, we will relax the local thermodynamic equilibrium (LTE) assumption in photospheres and chromospheres. In general, hydrostatic equilibrium will be valid everywhere. Radiative equilibrium is valid in the photosphere, but this will no longer be the case in the chromosphere. Some velocity fields are, in this context, sometimes "ad-hoc" parameters, existing for empirical purposes only. In reality, our knowledge of turbulence

in these stars is meager; the empirical curve-of-growth microturbulence is, in general, inconveniently supersonic in some outer layers.

The Mira characteristics (M. Querci, this volume), which will be discussed in the section *Shock-Wave Gas Dynamics and Pulsation Theory*, are more appropriate for a nonthermal concept. In this case, the velocities are no longer ad hoc parameters, and the shock-wave velocities that can exist in those stars are large enough to produce aerodynamic dissipation. In any case, the complete nonthermal models for Mira and non-Mira-type giant and supergiant cool stars will be obtained in the future when a consistent solution of the dynamic-transfer problems will be found.

Another important characteristic of the present models is that they are one-component models, and the probable existence of surface inhomogeneities is not taken into account. We know that large inhomogeneities exist in the atmospheres of the Sun and of the late-type dwarfs. Giant cells are predicted to exist in the late-type giants (Schwarzschild, 1975), but to the present time, no satisfactory observational evidences of these cells have been advanced (see, for example, Johnson, this volume). One possibility for future development of multicomponent atmospheric models can be made by a simultaneous diagnosis of the hotter and cooler components of the atmosphere, for instance, by the Mg II emission and by the CO fundamental vibration and rotation bands, respectively. (See Heasley et al., 1978, for an analogous study of Arcturus.)

Two main regions are important for these stars: the photosphere and the chromosphere. In view of the observational evidence of the absence of a high-temperature plasma, no transition regions and coronae are considered. The section *Photospheres* is devoted to the discussion of non-LTE effects in photospheres. In the section *Chromospheres*, we discuss the recent research on the chromospheres of these types of stars. In the section *Shock-Wave Gas Dynamics and Pulsation Theory*, we discuss elementary shock-wave and pulsation theories and their applications to Mira long-period variables.

PHOTOSPHERES

Our approach to the study of quasi-thermal photospheres will consist of relaxing the LTE hypothesis. In the subsection *Kinetic Equilibrium Line Formation*, we consider the non-LTE line-formation theory in photospheres. In the following subsection, we will discuss the metal ionization equilibrium and an application to a typical carbon-rich star photosphere.

Kinetic Equilibrium Line Formation

The main purpose of this subsection is to calculate a theoretical stellar spectra starting from a given atmospheric model representing the photosphere. This model consists essentially of a distribution in height of the kinetic temperature, gas and electronic pressures, and continuum opacities. The validity of the Maxwellian velocity distribution of particles provoking the collisions is assumed. Non-LTE line formation using this assumption has received the name "kinetic equilibrium" (KE) line formation (Athay, 1972).

Statistical Equilibrium. By definition, the statistical equilibrium equation relates the population numbers of different levels of the atom (n_i) to the rates causing changes in this population. Note the important assumption that $dn_i/dt = 0$. Considering an atomic model of N bound levels and a continuum (k), the statistical equilibrium equation can be written as:

$$n_i\left(\sum_{l=1}^{N} P_{il} + P_{ik}\right) = \sum_{l=1}^{N} n_l P_{li} + n_k P_{ki} \quad , \tag{8-1}$$

where $P = R + C$, and R and C are the radiative and collisional rates, respectively. The

upward rate is the excitation between two bound levels (i, l) or the ionization for a bound-free transition (i, k). The respective inverse processes are the deexcitation and recombination. The total number density of the atom is given by the particle conservation equation,

$$n_{tot} = \sum_{l=1}^{N} n_l + n_k \quad , \qquad (8\text{-}2)$$

where n_k is the number density of ionized atoms. Assuming that n_{tot} is known and that the total rates can be calculated, the equations can be solved to find the populations n_l and n_k.

The radiative photoionization and recombination rates depend on the mean intensity of radiation J_ν by the following expression:

$$R_{lk} = 4\pi \int_{\nu_{kl}}^{\infty} \frac{1}{h\nu} a_l(\nu) J_\nu d\nu \quad , \qquad (8\text{-}3)$$

where $a_l(\nu)$ is the photoionization cross section and ν_{kl} is the ionization threshold frequency.

If $J_\nu = B_\nu(T_e)$, B being the Planck function, the recombination rate can be calculated (see, for example, Mihalas, 1978) by

$$R_{kl} = \frac{n_l^*}{n_k^*} R_{lk} \quad , \qquad (8\text{-}4)$$

where n^*_l/n^*_k is given by the known Saha-Boltzmann equation. Knowing the collisional ionization rate, C_{lk}, a relation similar to (8-4) can be used to calculate the collisional recombination rate, C_{kl}. Radiative and collisional excitation rates can be calculated by classical relations using the Einstein radiative coefficients and Maxwellian distribution of level populations (see also Mihalas, 1978).

For two levels i and j, the line-source function is defined as:

$$S_L = \frac{2h\nu_{ij}^3/c^2}{\frac{g_j}{g_i}\frac{n_i}{n_j} - 1} \quad , \qquad (8\text{-}5)$$

g being the statistical weight. This last expression can always be written in the form (using relation (8-1)):

$$S_L = \frac{\int \Phi_\nu J_\nu d\nu + \epsilon B'}{1 + \epsilon} \quad , \qquad (8\text{-}6)$$

Φ_ν being the normalized absorption profile. This expression contains three fundamental physical processes: (1) the diffusion term, $\int \Phi_\nu J_\nu d\nu$, (2) the source term or creation of line photons, $\epsilon B'$, and (3) the sink term or destruction of line photons, ϵ.

Transfer Equation. In reality, S_L and J_ν are related by the equation of radiative transfer, measuring the change in distance of the intensity of radiation I_ν, making an angle θ ($\mu = \cos\theta$) with the normal to the surface:

$$\mu \frac{dI_\nu}{dz} = -k_\nu (I_\nu - S_L) \quad . \qquad (8\text{-}7)$$

If we write the line-absorption coefficient as $k_\nu^L = k_o^L \phi_\nu$, where $\phi_\nu = \Phi_\nu / \Phi_o$, we obtain the total monochromatic optical depth defined by:

$$d\tau = (\phi_\nu + r_o)\, d\tau_o \quad , \qquad (8\text{-}8)$$

where $d\tau_o = k_o^L\, dz$ and $r_o = k^C/k_o^L$. The transfer equation is then written as:

$$\mu \frac{dI_\nu}{d\tau} = I_\nu - S_t \quad , \qquad (8\text{-}9)$$

S_t being the total source function.

$$S_t = \frac{\phi_\nu S_L + r_o S_C}{\phi_\nu + r_o} \quad , \qquad (8\text{-}10)$$

where C refers to the continuum. The line-source function S_L, as written in relation (8-6), admits the validity of the complete redistribution of line photons (i.e., the emission profile is equal to the absorption profile). S_L is then not frequency-dependent. The main goal of the KE line formation consists of solving simultaneously the statistical (8-6) and transfer (8-9) equations, specifying the boundary conditions and the geometry of the medium.

Applications of KE Line Formation in LTE M–C Photospheres

Very few works have been devoted to the KE line formation in photospheres of late-type giants and supergiants of the M–C type. This is not the case of the slightly hotter stars of type G and K, which have received much more attention. Regarding the cooler types, the main work is related to the abundance determination of lithium. The importance of this element as an indicator of the internal and atmospheric evolutionary state of these stars is well known. Due to the relative ease of creation and destruction of this element, very large abundance differences can be found in these stars. These abundances vary from values smaller than the solar abundance to the extremely large values found in the "super lithium" C stars: WZ cas, WX Cyg, and T Ara. In the latter case, Li can no longer be considered as a trace element. However, abundances for these stars are not well known because they depend on solutions of the excitation/ionization problem described above, and these are not yet available.

Lithium Line Formation of M–C Giant Photospheres. Recent work on Li abundance determination in M-type photospheres has been undertaken by Luck and Lambert (1982), using improved observational data and based on model photospheres taken from the grid of Johnson et al. (1980). They used the complete linearization KE method code (Auer et al., 1972) to calculate the non-LTE abundance of Li with an atomic model of four levels plus continuum (Luck, 1977). Using an empirical solar line blanketing adapted to late-type giants, they found no non-LTE effects giving abundance differences for Li larger than 0.1 dex, suggesting that, because of the reduction of the ionizing field by line blanketing, non-LTE effects are not important in the ionization balance of Li in early M giants and supergiants. This work is based on the resonance Li I line at λ6708. It would be desirable for future Li studies to attempt to observe and use the subordinate Li I line at λ6103. This weak line has been identified by A. M. Boesgaard (Merchant, 1967) in early high-luminosity M stars.

Concerning the carbon-enriched photospheres, de la Reza and Querci (1978) performed KE calculations for the neutral lithium lines. The method they employed for solving the radiative and transfer equations is the integral flux divergence method (Athay and Skumanich, 1967; Athay, 1972). An atomic model of four levels and a continuum was also used. The photospheric LTE models were taken from the grid calculated by Querci (1972) and Querci and Querci (1975). The effective temperatures had values between 3800 and 3500 K, $g = 10$, C/O = 1.3. The photoionizing radiation field and the abundance were considered to be free parameters. The radiation field had the purpose of mimicking the effect of possible chromospheres and of simulating more or less blanketing. The main results were:

1. Li I is almost completely ionized in all models with $T_{\text{eff}} > 3500$ K.
2. The ionization is increased in KE.
3. $S_L > B_\nu(T)$ in the line-forming region, except for the case of the resonance λ6708 line with an Li abundance equal to 10^{-8}.
4. Profiles are sensitive to Li abundance and the chromospheric radiation temperatures, but not to the possible presence of graphite grains in the temperature minimum region.

5. Appreciable differences between KE and LTE were found for λ6708 only, although the Li I line at λ6103 is useful for distinguishing the effects of abundance from those of the chromospheric radiation field.

6. In LTE, to produce lines of Li I as strong as those observed in the lithium-rich C stars without enhancing the Li abundance, would require $T_{\rm eff}$ 2600 K.

Future Li abundance analysis should probably take into account aspects that have not been considered in the past: heterogeneities and spherical symmetry. Recently, Giampapa (1984) found that an enhanced chromospheric activity, such as a solar plage, can diminish the equivalent widths (W_λ) up to a factor 2 due to the increased ionization. This agrees with the observed anticorrelation found between the increase of emission of Ca II K line and the W_λ of the λ6707 Li line in the Sun. Special care must be taken when the Li I λ6707 line is compared to lines of Ca or Na as, for example, to the neighbor line of Ca I at 6717 Å. A proper KE analysis must also be made for these comparison elements.

Steenbock and Holweger (1984) investigated the ionization effect of the ultraviolet radiation field shortward of 3500 Å, which controls the ionization balance of Li. The thermalization effect of the H–Li atomic collisions was also estimated. In the case of a typical galactic disk late-type supergiant, the non-LTE effect measured by $\Delta\log\epsilon = \log\epsilon - \log\epsilon$ (LTE) can be equal to 0.57. This value is reduced by a factor of 2 if line blocking is considered. Due to the low densities involved, the thermalization collisions with H atoms have a negligible effect. For late-type halo giants of smaller metallicity, the results are similar; however, due to the larger densities, the thermalization collisions can be somewhat more important. To examine the influence of W_λ on the Li abundance, a careful comparison must be made between the works of Steenbock and Holweger (1984) and Luck and Lambert (1982). Also, spherical symmetry must be taken into account, particularly in the case of late-type supergiants.

KE Line Formation of Molecules. The KE problem of line formation for molecules in stellar spectra can be significantly more complex than that for atoms. In fact, the analysis must contain all the rates of formation and destruction of molecules. In some cases, the destruction process, such as photodissociation of molecules, can be a minor process in the statistical equilibrium (i.e., the case, for example, of the important molecules TiO and SiO in M stars and CO and CN in C stars). These molecules have large dissociation energies, and the corresponding radiation for photodissociation is located in the ultraviolet ($\lambda < 1500$ Å), which is very low in these stars, especially in the C stars.

Other considerations that limit the applicability of this analysis are the poor knowledge of the cross sections involved and the numerical intractability of the calculation of a band formed by hundreds of molecular lines. An interesting and general work on these problems is presented by Hinkle and Lambert (1975). Another work related to the formation of CO is that of Thompson (1973). The main conclusions of Hinkle and Lambert are as follows:

1. Because of the domination of the collisional process, LTE line formation ($S_L = B$) is the appropriate form for vibration/rotation transitions occurring within the ground electronic state. (These are the transitions found in the infrared spectra.)

2. The equilibrium of the excited electronic state is radiatively controlled, especially for late-type supergiants. These lines would be formed by the scattering process ($S_L = \int \Phi_\nu J_\nu d\nu$). For an optically thin absorption line, $S_L = J_\nu^c$, where J_ν^c is the local mean intensity in the continuum. (These transitions are found in

the visible and near-infrared stellar spectral regions.)

For the thin-line approximation, the equivalent widths will depend on the ratio, J_ν/B_ν, which can be very high in the outermost layers of stars. The equivalent widths will then be lower than those calculated in LTE. However, for the lines that are not optically thin, the line-source function depends on the scattering term, $\int \Phi_\nu J_\nu d\nu$, and the continuum source function. The line formation will be nonlocal in nature, and the complete KE equations must be solved. This complete KE calculation has been made by Mount et al. (1975) and Mount and Linsky (1975) for the violet CN band in the Sun and α Boo and by Carbon et al. (1976) for the fundamental bands of CO in cool stars. All these investigations found significant departures from LTE. For late-type stars, $S_L < B$ has been found. Contrary to the thin case, these results give stronger absorption lines in KE than in LTE.

The electronic bands, as is the case of CO, can be found in the ultraviolet. Ayres et al. (1981) showed evidence of the presence of fluorescent spectra of CO bands pumped by chromospheric emissions of O I at λ1380 and C I at λ1600. These bands appear as weak emissions near the C II (λ1335) and C IV (λ1550) features, which are normally indicators of the presence of a hot gas at 10^5 K. These authors then call for caution in the interpretation of these features in red giants.

Ionization Equilibrium in Photospheres

Non-LTE effects have always been suspected to exist in the atmospheres of late-type giant and supergiant stars due to their low total densities. However, rather than the total density, it is the free electron density which is important, because of its contribution to the excitation/ionization collisional process and to the continuous opacity. The goal of the study of ionization equilibrium is to determine the real distribution and effects of the electron density produced by the electron donors. In cool stellar photospheres, instead of H, which is the fundamental electron donor in chromospheres, the most abundant metals with low-ionization potentials are the principal sources of electrons. These are principally K, Na, Al, Mg, and Ca.

In this respect, very little study has been directed to these interesting problems in the photospheres. We can cite only two investigations: the theoretical work of Auman and Woodrow (1975) and the empirical work of Ramsey (1977, 1981). Ramsey compared the observed ratios of the equivalent widths of the [Ca II] λ7323 and Ca I λ6573 lines with those calculated by LTE model atmospheres of late-type supergiants. A certain discrepancy of these ratios begins to be detected for models cooler than 4250 K. This could be interpreted as evidence of non-LTE effects. However, as Luck and Lambert (1982) show, the continuum placement in these spectral regions is difficult, suggesting an inadequacy of the apparent local continuum of Ramsey. Nevertheless, we must not be far from reality, and as the theoretical work of Auman and Woodrow show, there are clear indications of non-LTE effects in high-luminosity cool stars. These authors iteratively solve the atmospheric equations with only the statistical equilibrium of the metallic electronic donors mentioned above. The simplifications are: (1) no radiative transfer is assumed, (2) the bound-bound transitions are treated in radiative detailed balance, and (3) no atomic or molecular (with the exception of H_2O) blanketing is taken into account. Even with these simplifications, their work was a fundamental step in this type of research.

To discuss the basic features of the ionization equilibrium, we consider the simplest case of a one-level atom with a continuum. The statistical equilibrium (see Equation (8-1)) is then:

$$n_l (R_{lk} + C_{lk}) = n_k (R_{kl} + C_{kl}) . \quad (8\text{-}11)$$

Using Equations (8-3) and (8-4) and the Saha-Boltzmann relation, Equation (8-11) can

be solved to give the value of the departure coefficient, b, which is given by:

$$b_l = \left(\frac{n_l}{n_l^*}\right) \Big/ \left(\frac{n_k}{n_k^*}\right) \quad . \tag{8-12}$$

When the atoms are predominately neutral, almost all atoms are at level 1; therefore:

$$b_1 \sim n_k^*/n_k \, , \tag{8-13}$$

and when atoms are strongly ionized, $n_k \sim n_k^*$, b is reduced to:

$$b_1 \sim n_1/n_1^* \, . \tag{8-14}$$

Actually, the mean intensity, J_ν, appearing in Equation (8-11) is also a function of b_1, and the expression relating J_ν to b can be found by simultaneously solving the statistical and transfer equations (KE). Since the line-absorption coefficient is also a function of n_l and b_1, an iterative process must be used to solve the equations for the values of b_1. Due to the low electron densities existing in the atmospheres of late-type giants, the value of b_1^{-1} depends exclusively on the ratio J_ν/B_ν. (For an explicit form of Equation (8-12), see Avrett and Loeser, 1969.) This ratio may be very large in the outermost regions due to the large values of the Rayleigh scattering coefficient compared to the other continuous opacities, especially in the ultraviolet. In the deeper layers, the ratio, J_ν/B_ν, converges to unity, giving a departure coefficient b_1 equal to unity.

A practical form to express the ionization equilibrium is (Auman and Woodrow, 1975):

$$\left(\frac{N^+ N_e}{N}\right)_{\text{KE}} = \frac{U^*}{U} \left(\frac{N^+ N_e}{N}\right)_{\text{LTE}} \, , \tag{8-15}$$

where N^+, N, and N_e are the ion, neutral, and electron densities. U and U^* are the partition functions assuming KE and LTE, respectively. It is easy to see that, in general, $b_1^{-1} \simeq U^*/U$. Assuming the neutrality of the plasma, the new electrons can be calculated by means of the new ion density. This "new" model can be iterated to obtain new values of J_ν which can be used again in the KE calculation. This iterative process can be used until convergence in the departure coefficients is obtained.

To illustrate the behavior of the b_1 values in model photospheres, we have calculated the KE for neutral atoms of K, Na, and Mg (for 5, 4, and 5 bound levels, respectively). These calculations consist of finding the first values of U^*/U, using the mean intensities J_ν from an LTE molecular-blanketed model photosphere. The model chosen is that of Querci (1972) and Querci and Querci (1975) corresponding to $T_{\text{eff}}/g/$ratio of C/O equal to 3400/0.1/3.26. Because no atomic line or grain blanketing was considered in those models, the J_ν values, especially in the ultraviolet, are maximum values. The U/U^* obtained, then, expresses maximum departures from LTE. It is important to mention, however, that subsequent iterations with model calculations will reduce, even more, the b_1 values. These results are presented in Figure 8-1.

We have experimented numerically to gage the sensitivity of U^*/U to the changes of J_ν values at different continua. We find that a reduction in J_ν by a certain factor for the first excited levels of all atoms produces a reduction of approximately the same factor in the values of U^*/U. These results are also sensitive to the second excited state of Mg I (as also found by Auman and Woodrow, 1975). We have examined the abundance effects by arbitrarily changing the model abundances for K and Na. Although there are no significant changes in the J_ν values of the LTE model, the KE populations of the bound levels change, giving larger departures for smaller abundances.

The converged values of Auman and Woodrow do not show significant temperature changes from the initial models. The most important changes are found in the electron density for the models: $T_{\text{eff}} = 2500$ K, $\log g = 0.0$, and $T_{\text{eff}} = 2000$ K, $\log g = -1.0$, in which

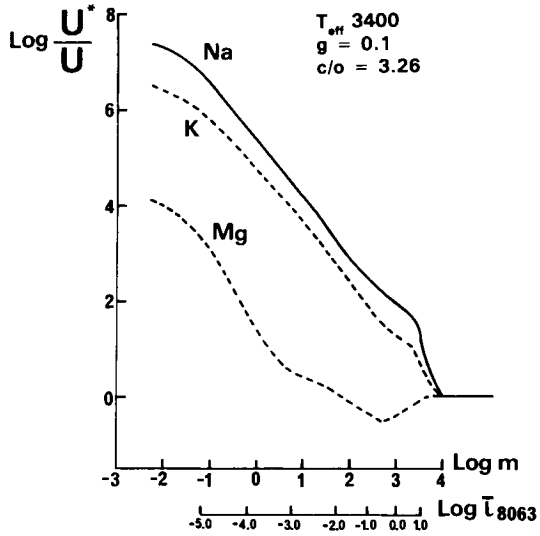

Figure 8-1. Behavior of the ratio of the initial partition functions with depth in the photospheres of a carbon-star model and for the principal electron donors, K, Na, and Mg. m is the column mass. A scale of depth for the reference wavelength, λ8063, is also shown.

the electron pressures increase in the outer layers, compared to LTE models, by factors of 14 and 60, respectively. Only slight changes are found in the continuous opacity (in general, less than 5 percent). This is due to the fact that, in the outermost layers where the non-LTE effects are larger, the continuum opacity is controlled by Rayleigh scattering by atomic and molecular hydrogen (especially in the ultraviolet), which is independent of Ne. Of course, H^- is an important source of the continuous spectra in these stars, and it depends on Ne. However, H^- appears to be important only in deeper layers in which the non-LTE effects are smaller. It is also important in this respect that a complete calculation of the H^- equilibria be performed following the suggestions of Lites and Mihalas (1984).

We conclude that non-LTE effects found for the carbon-star astmospheres shown in Figure 8-1 are large. These maximum values, however, are partial and will be reduced by iteration with the model. We hope that future models will contain blanketing by atomic lines (and grains?) to enable construction of reliable non-LTE blanketed atmospheres.

CHROMOSPHERES

The chromospheres of noncoronal stars such as M and C high-luminous stars are regions that lie immediately above the photospheres and in which a large part of the nonradiative energy available heats and expands the gas in order to produce an extended warm region. It is in these regions that the mass loss begins to take place.

Nevertheless, it is precisely in this type of star that real atmospheres seem to be much more complicated than in our simple models. That is due to the presence of a number of physical processes involved (e.g., abundance and grain effects, weak and strong shock waves, magnetohydrodynamic waves, turbulence, and possible large convection effects). Although a realistic energetic budget will be difficult to calculate under these conditions; it is the only way to understand why some stars have different kinds of chromospheres. (See Linsky, 1984a, for a recent review on chromospheres of non-Mira M and hotter G- and K-type stars.)

Hydrogen Ionization

In photospheres, ionization of abundant low-ionization metals was important, whereas in chromospheres, the ionization role is played by hydrogen. In fact, even at the modest temperatures, between 4000 and 10000 K, which exist in these zones, hydrogen will be ionized. Ionization of helium is less important, since it will be produced only at higher temperatures.

The construction of chromospheres must then calculate simultaneously the H line and continuum formation, together with the atmospheric equations using methods, for example, like those developed by Avrett (for a recent paper, see Avrett, 1985). H continua can also be treated by a method developed by O'Brien (1980) using the code (LINEAR) of Auer et al. (1972; see also Auer, 1973). This last procedure can be modified to treat H lines also.

Regarding H, another interesting problem that should be mentioned is the puzzle of the H_2 quadrupole line in M and S stars (Tsuji, 1983) and in C stars (Goorvitch et al., 1980; Johnson et al., 1983). The strongest infrared H_2 quadrupole line is not detected in non-Mira M stars, contrary to the theoretical expectation which predicts an increasing strength of this line as we go to cooler stars (Tsuji, 1983). This H_2 feature is clearly observed in S-type Mira stars (Hall and Ridgway, 1977; Tsuji, 1983). In C stars, the line is present in Mira variables.

Tsuji (1983) and Johnson et al. (1983) describe the principal physical scenarios that could explain the presence or absence of this line. Even if the problem between M and C stars appears to be similar, it is not clear whether the explanation will be the same for both types of stars.

Lower surface temperatures produce a stronger H_2 line if we consider the thermal sensitivity of the line. Spherical symmetry can produce these lower temperatures (Schmid-Burgk et al., 1981). This effect could thus explain the presence of H_2 in S stars. Tsuji (1983), however, favors the explanation of lower surface temperatures in S stars in respect to M stars (differences between 150 and 350 K), produced by the more efficient cooling effect of CO in S stars. Nevertheless, the problem concerning the non-Mira M stars remains open. Unless a general revision of the temperature scale is made, other mechanisms, such as the presence of a chromosphere, particularly on later types, could be invoked to explain the destruction of the H_2 molecules.

It is possible that the puzzle has an explanation other than thermal sensitivity for the case of C stars. Johnson (see Chapter 7) suggests the possibility of hydrogen deficiency in C stars. This suggestion is strengthened by an important characteristic of C stars (i.e., the absence of Balmer lines in N carbon stars (Yamashita, 1972, 1975)). Another fact that suggests an H deficiency is the weak observed emission peak of H^- at 1.6 μm in N stars as compared to that predicted by models (Goebel and Johnson, 1984). These authors propose that, if H deficiency is real in N carbon stars, this can be explained by an episodical ejection of an H-rich shell. That conclusion has important consequences for the evolutionary study of these objects and the chemical evolution of galaxies. It is important in this respect, however, to calculate the H^- equilibrium in the most complete way, following the treatment given by Lites and Mihalas (1984). Perhaps we could explain the absence of Balmer lines in N stars by the mechanism put forward by them, in which charge neutralization processes decrease excited H-level populations in favor of protons and H^- ions affecting the H ionization and the Balmer lines.

Bifurcated Chromospheres

The behavior of such important heating and cooling sources as H^-, CO bands, and metallic lines in stellar gases at the minimum solar temperature region, $T_{min} \simeq 4000$ K, has introduced new ideas on the structure of the solar chromosphere (Ayres, 1981). For the latest discussions, see Ayres (1985) and Avrett (1985). We think it will be interesting to check whether these concepts can be applied to future studies of detailed late-type star atmospheres.

First, let us examine the mechanisms: from one side, CO cooling is important for temperatures lower than 4000 K. For $T \gtrsim 4000$ K, the molecule dissociates, and its cooling effect diminishes. (The role of CO as a cooling source in late-type stars has been discussed initially by Johnson, 1973.) On the other hand, at this $T_{min} \simeq 4000$ K region, H^- is contrary a heating source due to photodetachment. H^- will be converted in a coolant only at higher temperatures near 5000 K. Bearing this in mind, we can now describe the principal physical idea (Ayres, 1985). For temperatures near 4000 K in a stationary atmosphere, the cooling properties of CO can act against the heating produced by H^- and the deposition of nonradiative energy, maintaining a cool gas at $T \simeq 4000$ K up to higher zones which were classically defined as belonging to the chromosphere.

However, in some supposedly restricted areas of the photosphere surface (e.g., magnetic flux tubes), the deposition of nonradiative energy can be strong enough to destroy the CO molecule and produce a temperature inversion that forms a localized chromosphere, for which the classical T_{min} concept can be applied. This stationary atmosphere will then be a two-component thermal atmosphere in which two zones—one hot, the other cold—will coexist at the same height. This type of bifurcated model can also be explained by nonstationary atmospheres (Muchmore and Ulmschneider, 1985) in which waves produced hot compressed zones and rarefied cool zones cooled further by CO radiation. Kneer (1983) has also examined the possibility that the thermal instability of optically thin infrared vibration/rotation bands of CO could produce chromospheres of late-type stars, proposing an interpretation of the known Wilson-Bappu effect (Wilson and Bappu, 1957).

One of the purposes of these bifurcated models is to reproduce the ionic emission as Ca II K simultaneously with the radiation of the CO infrared band. The empirical basis of these models is presented in Ayres (1985). Future development will depend, as Ayres explains, on a detailed treatment of non-LTE effects of CO, especially for ultraviolet electronic transitions. Metallic blanketing will be important because non-LTE effects will not only decrease the cooling effects of metals by a large factor but will also increase their effectiveness in depth by a similar factor (Kalkofen, 1985).

We would like to emphasize that it will be interesting to investigate the application of bifurcated models to late-type stars for which simultaneous observations of metallic emission lines and CO bands have been made.

Chromospheres of M-Type Stars

Observational Evidences. The research on chromospheres in M-type giants and supergiants has been based on the presence of some emission lines (see, for example, M. Querci, this volume) like the Mg II and Ca II resonant lines (Basri et al., 1981; Hagen et al., 1983) and Fe II lines (Boesgaard and Magnan, 1975; Boesgaard, 1979). Other lines also appearing in emission are the hydrogen Balmer lines (Jennings and Dyck, 1972; Hagen et al., 1983) and the Hϵ line (Wilson, 1957, 1982). However, the hydrogen lines can be explained by other mechanisms (e.g., shock waves). In the ultraviolet, research is also concentrated on the C II lines.

Dyck and Johnson (1969) and Jennings and Dyck (1972) first showed an anticorrelation between the H and K lines of Ca II and the infrared excess and polarization, characterizing the presence of dust grains in their atmospheres. This anticorrelation was interpreted by Jennings (1973) as due to a quenching effect by dust grains. These grains would radiate the nonthermal energy, preventing the formation of a chromosphere. This anticorrelation has also been found by Hagen et al. (1983) in a relatively large sample of M stars. However, the results of Hagen et al. show a difference in the sense that the real anticorrelation of Ca II emission is not with circumstellar dust, but appears to be with a dust-to-gas ratio (the degree of grain condensation). The core emission of the Ca II lines disappears in the coolest stars having strong dust-to-gas ratios. That is the case, for example, for the stars, HD 207076 (M7 III) and R Dor (M8 III). We can infer that these stars probably do not possess a chromosphere. However, any conclusion must be analyzed in detail because R Dor also shows Mg II in emission, which is normally considered as a chromospheric indication. Hagen et al. suggest a possible shock origin for this Mg line. This shock origin is also suggested for the Balmer emission lines that appear only in stars with high dust-to-gas ratios (Jennings and Dyck, 1972; Hagen et al., 1983).

Extension of the Chromospheres. Recent work based on the ultraviolet (UV) C II emission lines has permitted an empirical estimate of the temperatures, electronic densities, and geometric extensions of chromospheres of luminous stars of spectral types between G9 and

M3. The C II lines involved are the resonance triplet (UV 1) at 1335 Å and the multiplet (UV 0.01) at 2325 Å. Stencel et al. (1981) showed that, for electronic densities between $10^7 \leq N_e \leq 10^9$ cm^{-1}, the line ratios of the multiplet, UV 0.01, can be used as an indicator of N_e. The electronic temperatures are obtained by comparison of the observed ratios of the UV 1 and UV 0.01 total fluxes, together with a theoretical calibration of this ratio with N_e and T_e like that of Hayes and Nussbaumer (1984). Brown and Carpenter (1985) introduced this technique to obtain the temperatures of the C II line-emitting regions in several luminous late-type stars, assuming that the radiation arising from both multiplets came from a region of constant N_e. For M stars, the chromospheric values are $N_e \sim 10^8$ cm^{-3} and 7000 K $\leq T_e \leq$ 9000 K. The most interesting estimations are, however, those related to the sizes of these chromospheric C II emission regions. The most recent results are those of Carpenter et al. (1985), obtained by using the observed total fluxes of multiplet UV 0.01, the above-mentioned values of N_e, T_e, the photospheric radii, R_*, and the angular diameter, ϕ_*. The mean thickness of the emitting region, L, is calculated by these authors by the relation:

$$L = \frac{f_{2325}}{\Lambda E} \quad , \tag{8-16}$$

where Λ is the solid angle subtended by the chromosphere and E is its volume emissivity given by:

$$E = \frac{1}{4} N_e N_{\mathrm{C\,II}} C_{12} h\nu_{21} \quad . \tag{8-17}$$

The number density of C II can be calculated by:

$$N_{\mathrm{C\,II}} = \frac{N_{\mathrm{C\,II}}}{N_{\mathrm{C}}} \frac{N_{\mathrm{C}}}{N_{\mathrm{H}}} \frac{N_{\mathrm{H}}}{N_e} N_e \quad , \tag{8-18}$$

for which the expression of fractional ionization of C and H and C abundance must be known. The solid angle is expressed in terms of the chromospheric radius, R, and the values of R_* and ϕ_*. The principal unknowns, L and R, are then related, and an iterative technique is used. These estimations, although subject to uncertainties, as values of N_e and the C abundance, clearly show that late-type giants with coronal regions (G9 and K0) have very thin chromospheres, with $R < 0.1$ percent of the photosphere. Noncoronal stars like M giants and supergiants have instead, on the average, chromospheric emission regions extending out to 2.5 photospheric radii. In the case of the M star, α Ori, for example, this method gives a chromospheric radius smaller by a factor of 2 than that found by Newell and Hjellming (1982) using radio observations. Of course, one must consider that the assumption of constant N_e is quite simplistic.

Thus it appears that these red high-luminosity stars contain a vast chromosphere extending to several stellar radii many times larger than their isothermal pressure scale heights. Mass loss is bound to be happening in these regions. Kinematically speaking, the chromospheres could, in a way, be physically detached from the photospheres (Goldberg, 1979). How can these extended chromospheres be produced? Certainly, the mechanism of thermal evaporation, which works in a hot stellar wind, will be inoperative here, due to the low temperatures and thermal pressures involved. In addition, it is not clear whether radiation pressure impinging on molecules (Maciel, 1976, 1977) or Lα radiation (Wilson, 1960; Haisch et al., 1980) could produce those extended regions by gas levitation and expansion. This will require further study. Other pressures of turbulent or magnetic origin can also be invoked. Stencel (1982b) mentioned that an rms turbulent velocity of the order of 50 km s^{-1} would be necessary to support material with a density of 10^8 cm^{-3} at 5 stellar radii. A magnetic pressure of a modest magnetic surface field could produce this support (see Goldberg, this volume).

Line Formation in Extended Atmospheres. If

chromospheres extended to several photospheric radii, spherical geometry must be taken into account in any realistic treatment of line formation. In addition, chromosphere expansion effects must be considered if mass loss is taking place somewhere in these regions. Because wind outflow velocities of the order of 10 to 50 km s^{-1} are only a factor of 2 larger than typical microturbulence values in late-type giant stars, the Sobolev approximation that is valid for strong winds will probably be of no value. Recent numerical applications solve the transfer equation in a comoving frame for a spherical atmosphere in expansion, assuming a partial redistribution (PRD) of line photons (Drake and Linsky, 1983; Drake, 1985 (differential equation method); Avrett and Loeser, 1983 (integral equation method)).

For the photospheres, Equation (8-6) admitted the validity of the complete redistribution (CRD) function, in which the emission-line profile, Ψ_ν, is equal to the absorption profile, Φ_ν. This is no longer the case in the interpretation of strong resonance chromospheric lines. Here the PRD approximation represents an intermediate situation between the coherent scattering and the CRD (in which, contrary to the coherent case, no frequency relation exists between the incoming and outcoming photons). A recent numerical solution is presented by Hubený and Heinzel (1984) on the effects of PRD on subordinated lines.

The total actual probability of a photon of frequency ν being absorbed and reemitted at ν' is:

$$R(\nu,\nu') = \gamma R_{II}(\nu,\nu') + (1-\gamma)\,\Phi(\nu)\,\Phi(\nu'), \tag{8-19}$$

where R_{II} is the angle averaged probability, and γ is the coherence mixing fraction given by:

$$\gamma = \frac{\Gamma_{rad} + \Gamma_I}{\Gamma_{rad} + \Gamma_I + \Gamma_E}, \tag{8-20}$$

where R_{II} is the angle averaged probability, and γ is the coherence mixing fraction given by: inelastic deexcitation collisions, and elastic collisions (i.e., Stark and Van der Waals collisions).

Noncoherent scattering (CRD) is valid in the Doppler core, whereas coherent scattering is important in the inner wings. Absorption by continuum processes is important in the extreme wings. The difference between PRD and CRD has been discussed by Basri (1980) in static atmospheres and by Drake and Linsky (1983) in expanding chromospheres. The results of Drake and Linsky show, for example, that the increase of flow velocity and geometrical extension gradually transforms a double peak Mg II line into an approximate P Cygni Mg II line. Drake (1985) has described and applied the PRD techniques in a semiempirical way to interpret the Mg II line in Arcturus. However, no unique atmospheric model that explains the line profile has been found. As Drake mentions, it is important to make future tests of cooler giants that show other chromospheric line indicators. Also in this respect, it is instructive to compare the results obtained with those produced by pure theoretical models. For an extensive review paper on PRD stellar applications, see Linsky (1984b).

Model Diagnosis. Two different approaches are generally made to model chromospheric temperature, density, and velocity distributions. One is to calculate the KE of important resonance lines, usually Mg II and Ca II for various assumed chromospheric models, and then select the model which best fits the observed profiles. This semiempirical method has been applied by several workers in F-, G-, and K-type stars (see, for example, Linsky, 1980, 1981). Some elements of this methodology are presented in the section *Chromospheres of Carbon Stars*. The other approach is a theoretical one that consists of predicting a chromospheric model from an adopted nonradiative heating mechanism. This theoretical treatment has also been applied in the study of F-, G-, and K-type stars (Ulmschneider, 1979; Musielak and Sikorski, 1981). An important general theoretical work on this field is that of Athay (1981).

Very few detailed chromospheric studies of M-type stars exist, and to our knowledge, only the supergiant α Orionis (M2 Iab) has received special attention. Lambert and Snell (1975) first examined whether a simple nonextended constant-temperature chromosphere could contribute to the infrared excess observed in α Ori and in the semiregular variable, W Hydrae (M7-9). This contribution would be important only at wavelengths for which the silicate dust is a poor emitter. Isothermal chromospheres of 5000 and 8000 K were proposed for α Ori and W Hya, respectively. However, this kind of approach requires a detailed knowledge of the sometimes badly known dust properties. In addition, those chromospheres must now be placed in a huge CS region in which grains exist. New problems are now emerging as to determining the real distribution of grains in space and time in those huge atmospheres. Forming dust grains near the surface of α Ori also appears to be difficult (Draine, 1981).

Another approach in the study of chromospheres of M stars has been to analyze the velocity fields in α Ori (Boesgaard and Magnan, 1975; Boesgaard, 1979) and in the M2.5 giant, β Pegasi (Boesgaard, 1981); these studies were devoted to the formation of their strong Fe II emission lines in the 3100 Å region. The transfer problems are solved in a spherical moving atmosphere covering an extended region around the photosphere of the star. The line-source function is not specifically solved, but rather, it is parameterized in order to represent a chromospheric rise of the temperature. Finally, the optical depths are adjusted, by varying the velocity fields, to fit the observed profiles. One important result for α Ori is that the Fe II lines in this model are formed in a region that shows an infall of matter. The velocity changes from 15 km s^{-1} at 1.8 R_* (R_* is the stellar radii) to 60 km s^{-1} at the photosphere. In the giant, β Peg, the Fe II emission lines show a rather uniform outflow beginning at zero velocity at the photospheric surface and attaining 25 km s^{-1} at 2 R_*.

A more direct semiempirical approach to the chromosphere of α Ori has been undertaken by Basri et al. (1981), who fit KE partial redistribution calculations with the observed profiles of Mg II and Ca II resonant lines. The computed models are nonextended chromospheres in hydrostatic equilibrium, resulting in a plane-parallel atmosphere. These authors could not find a homogeneous chromosphere for α Ori that fitted both the Ca II and Mg II profiles. This preliminary model is shown in Figure 8-2.

Zarro (1984) has recently studied the possibility that the profiles of Balmer lines, such as Hα, could be chromospheric indicators in late-type giants. However, as we will see later in the section *Shock-Wave Gas Dynamics and Pulsation Theory*, H-lines can be formed in some M giants by processes other than chromospheric ones (i.e., strong shocks). Also in this respect, in N irregular carbon-type stars, the Balmer lines are extremely weak (Yamashita, 1972, 1975).

A different approach (theoretical) has been taken by Hartmann and Avrett (1983), who construct a model for α Ori by including the Alfvénic wave pressure to produce an extended chromosphere. The momentum and energy equations of the wind are solved for a radial steady spherical symmetric flow. The temperature, density, and velocity of the flow is then later computed to attempt to reproduce some observed features in α Ori. The temperatures are those resulting from the energetic balance of wave heating, adiabatic expansion, and radiative cooling.

The principal difficulty of this mechanism stems from our limited understanding of the dissipation of these waves. The geometrical scale in which this dissipation occurs is represented by the damping length, L. Considering L to be constant, the physical situation is very sensitive to the values of $\lambda = L/R_*$. If $\lambda > 1$, the theoretical terminal velocity of the wind greatly exceeds the observed values, whereas for $\lambda < 0.85$, no mass loss occurs, Hartmann and Avrett (1983) choose an intermediate constant value $\lambda = 0.9$ for their calculations. The two computed models are shown in Figure 8-2. The "high-expansion" curve corresponds to a model giving a mass loss

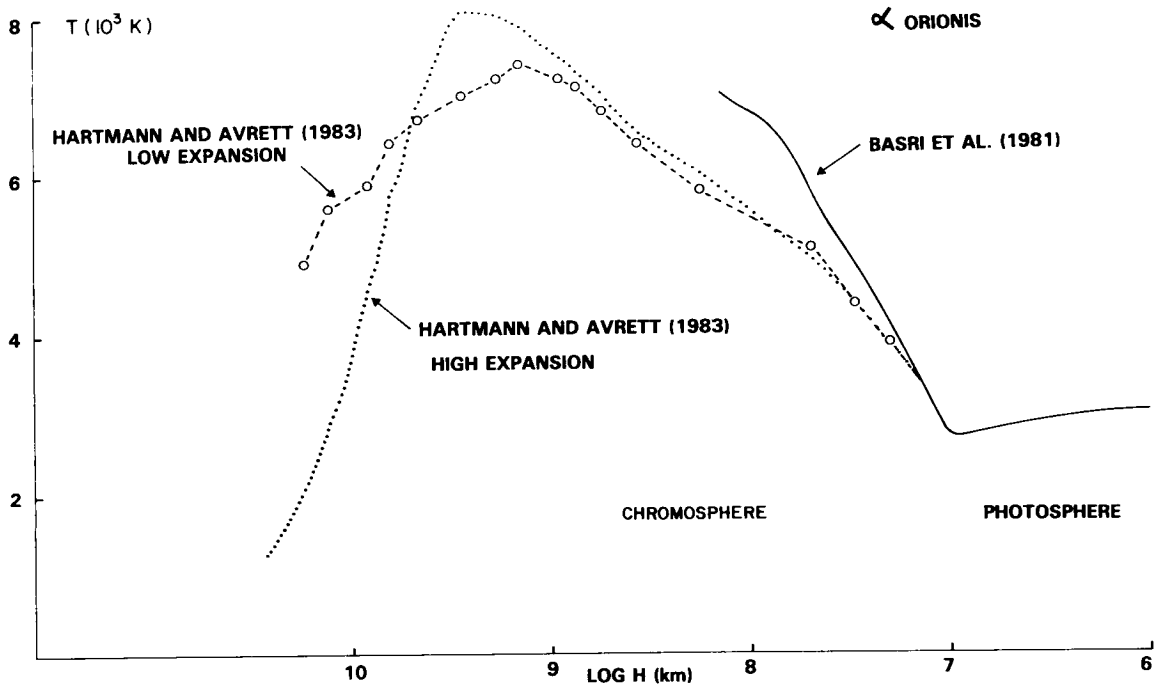

Figure 8-2. Temperature versus height chromospheric models of the supergiant M star, α Orionis. The nonextended semiempirical atmosphere of Basri et al. (1981) is shown, together with the theoretical extended models by Alfvén pressure waves (high and low expansion) of Hartmann and Avrett (1983). The photospheric zone is the same for all models.

equal to $1.4 \times 10^{-6} M_{\odot}$ yr^{-1}. The expansion velocities (V_{exp}) are of the order of 20 km s^{-1} and are larger than the turbulent velocities (V_{turb}). The other model, "low-expansion" with $V_{exp} < V_{turb}$, corresponds to a static energy equation. The photospheric model is the same as that of Basri et al. (1981). Both the high- and low-expansion models produce similar line and radio continuum emission in reasonable agreement with observations. Discrepancies with observations appear only when observed and computed profiles are compared. Theoretical profiles are much narrower than those observed. Predicted asymmetries are also too large. (The low-expansion model, however, produces nearly symmetric profiles.) In conclusion, larger V_{turb} and smaller V_{exp} by factors of 2 and 3, respectively, are necessary to match the observed data, suggesting a "quasi-static" extended chromosphere for α Ori.

Holzer et al. (1983) have criticized the use of a constant damping length. They believe that a more realistic interpretation will be one in which L is nonlinearly related to the state of the atmosphere (temperature, density, ionization, and radiative losses). They show that, if an ion-frictional damping is used in which the wave dissipation is produced by charge-transfer collisions between ions and atoms, it will give a thermal structure very different from that obtained by assuming constant L. These new temperatures are also the result of balance between heating by dissipation and cooling by radiation obtained in a self-consistent way. Holzer et al. (1983) also raise objections to the Alfvén wave mechanism as a general way to

produce cool massive low-speed winds for low-gravity stars. For them, any efficient mechanism (Alfvén waves or something else) must add the major part of the available energy in the subsonic region, without affecting the asymptotic flow speed u_∞. (u_∞ is much less than the escape velocity in low-gravity stars.) A small remaining energy will then be necessarily added to the flow in the supersonic region to guarantee the real escape of the wind.

Future modelers of α Ori must consider that time-dependent phenomena can be important input data. Although α Ori is a long-period variable (P = 2110 days), some rapid variations on a monthly scale have been observed (Goldberg, 1979). Other time-dependent phenomena could also be associated with possible large convective cells (Schwarzschild, 1975) or other mechanism, producing sporadic ejection of matter with velocities generally inferior to the escape velocity, so that infalling gas will be common, supporting perhaps the infall acceleration suggested by Boesgaard (1979). In addition, we cannot avoid the possible coexistence of hot and cool material producing an inhomogeneous multicomponent model.

Chromospheres of Carbon Stars

Although the presence of some Fe II emission lines in the violet appear to indicate the existence of chromospheres in N-type carbon stars, confirmation in certain stars (N stars) has come only recently through IUE observations of the 2200 to 3200 Å interval (Johnson and O'Brien, 1983; Querci et al.,1982; Querci and Querci, 1985), and in R stars by Eaton et al. (1985).

The stars observed by Johnson and O'Brien (1983) were all warm N-type stars, and none of them showed a strong violet depression. In fact, their ultraviolet spectra, beginning at 3200 Å, show a continuation of the photospheric spectrum with several absorption features down to wavelength λ2850, where the spectra appear to change and present emission lines. Here, two clear emission features are present that correspond to the Mg II and C II lines at λ2800 and λ2325, respectively. Because of the low resolution of IUE, the Mg II h and k lines are not resolved. The ratios f(Mg II)/f_{bol} obtained are, on the average, 100 and 25 times smaller than the respective ratios of K and early M stars. However, the ratio f(C II)/f_{bol} is only 2 to 4 times smaller than that of M giants. This difference is partially a consequence of the enhanced carbon abundance in carbon stars relative to M-type stars. The ratio f(Mg II)/f(C II) could be considered, in a way, to be independent of any superposed absorption. Even in this case, the latter ratio is 4 to 5 times smaller than that of M stars. From these results, Johnson and O'Brien suggest that chromospheres, weaker than those of M stars, must exist in these observed N-type stars.

How can the absence of light detection from other target stars be explained? Some of them have been integrated with exposure time up to 5 hours. Querci et al. (1982) explain this in two ways: one is the possible absence of a chromosphere. (This chromosphere could also be variable in time.) The other is the existence of a supplementary "ultraviolet depression." It is not clear if this supplementary opacity is or is not related to the classical violet depression that exists in some C stars and which begins at ~4200 A. At this point, it is important to note that the detection of light depends on the brightness of the star at U. Only the light of the brightest U stars like TX Psc and TW Hor were detected, whereas faint U stars such as YCVn and WZ Cas were not detected. This simple fact indicates that this is due to ultraviolet opacity of molecular and/or grain origin. (For a discussion of grains, see Lefèvre, this volume.)

Simple atmospheres can be formed by a photosphere and empirical plane-parallel ad-hoc chromosphere. When the photosphere is known, the chromosphere can be calculated using the following relations:

1. The hydrostatic equilibrium expressed by:

$$P - P_o = g(m - m_o) , \qquad (8\text{-}21)$$

where P_o and m_o are the total gas pressure and the column mass at the top of the chromosphere.

2. The total pressure given by the sum of partial pressures of the most abundant elements (in number N_{el})

$$P = n_H \sum_{l}^{N_{el}} (A_l + N_e) KT \ , \qquad (8\text{-}22)$$

where A_l is the abundance of the element l.

3. The charge neutrality,

$$N_e = N_p + N_H \sum_{l}^{N_{el}} A_l \frac{f_l}{1+f_l} \ , \qquad (8\text{-}23)$$

where N_p is the proton number, and each first stage of ionization is given by the function, f_l, between neutral elements and ions of the element, l. For H, the statistical equilibrium must be solved to obtain the departure coefficient, b_1, for the ground level. For H_e and other metals, ionization can be given by the Saha law.

We have four unknowns: N_H, P, N_e, and N_p for Equations (8-21), (8-22), and (8-23). The fourth equation must necessarily result from the energy-momentum conservation equation at any depth of the chromosphere. One way to replace it is to obtain an arbitrary relation between temperature and mass. One simple way is given by:

$$T = \alpha \log m + \beta \ , \qquad (8\text{-}24)$$

where α and β are constant coefficients determined from the boundary conditions: T_o at the top of the chromosphere and T_{min} at the minimum temperature region corresponding to the top of the photospheric model. All these equations can be solved by a rapid iterative process to produce the chromosphere.

The energy boundary conditions must be established for the fundamental variables, P and T: P_o, T_o and P_{min} and T_{min}. The choice of a smaller value of P_o will produce a more extended chromosphere for a given temperature gradient.

Using this method and keeping in mind the exploration of possible chromospheres of carbon stars, we have calculated some linear chromospheric extensions to the photospheric models of Johnson (1982). For these calculations, we have chosen two different carbon-enriched model photospheres with very different gravities and different effective temperatures. The main parameters ($T_{\rm eff}$/log g/ratio of C/O) are 3500/0.0/1.05 and 3000/2.0/1.02. For a chosen temperature distribution, the model will contain the calculated values of the column mass, the electron densities, and the departure coefficient, b_l, of the hydrogen. In the photosphere, b_l will be equal to unity. We have also calculated an ad-hoc depth-dependent microturbulence (increasing outward) by means of the following relation:

$$\xi = \alpha' \log m + \beta' \ . \qquad (8\text{-}25)$$

As boundary conditions for the top of the chromospheres, we have chosen a velocity that is somewhat smaller than the sound velocity and a zero velocity for the minimum temperature. (The published models of Johnson do not contain microturbulence velocities.)

For each photospheric model, we have calculated two linear chromospheres having different gradients. One corresponds to a "hot" model (T_o = 7000 K), and the other corresponds to a "cold" model (T_o = 4000 K). The boundary conditions are presented in Table 8-1, where P is the total pressure. The extension of the chromosphere, H_{chro}, is also contained in the table. For illustration, Figure 8-3 shows the behavior of the temperature versus column mass and the respective velocities.

KE Line Formation of the Magnesium Resonance Lines. In order to study the main

Table 8-1
Main Characteristics of the Chromospheres

Effective Temperature	Log g	P_o (dynes/cm^2)	T_o	T_{min}	H_{chro} (km)
3500	0.0	10^{-7}	7000,4000	2380	1.4×10^8
3000	2.0	10^{-5}	7000,4000	2010	9×10^5

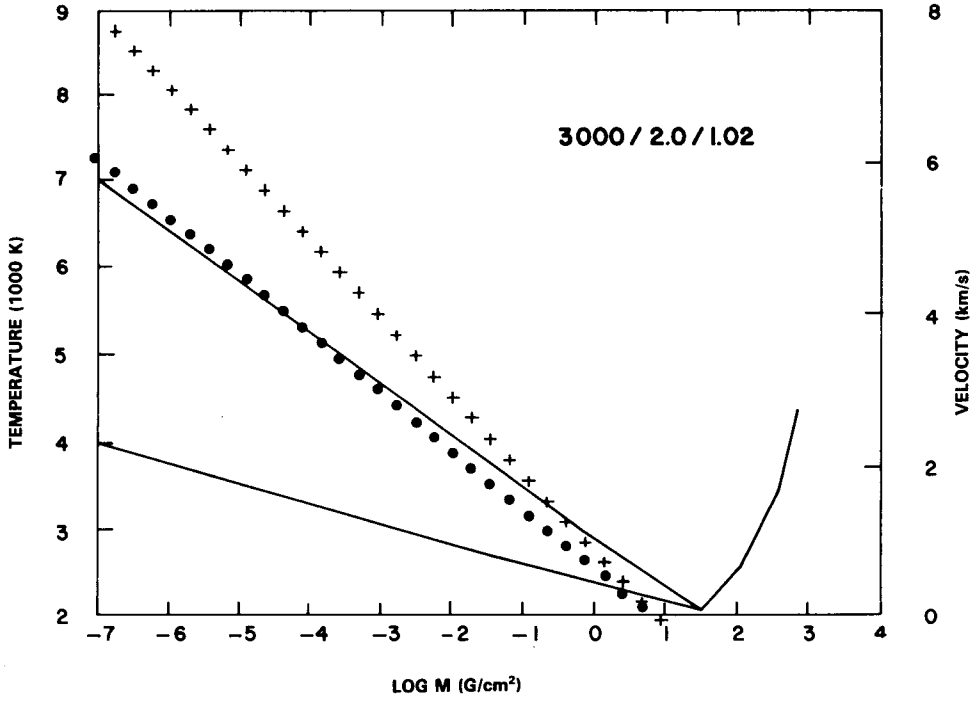

Figure 8-3. Distribution of temperature (solid lines) and velocities for the model 3000/2.0/1.02. Velocities for the hot chromosphere (T_o = 7000 K) are represented by crosses, and those for the cold chromosphere (T_o = 4000 K) by points.

characteristics of the presented atmospheric models, we have calculated the KE line formation of the resonance lines of Mg I at λ2852 and Mg II at λ2798. The latter line represents a mean of the h and k lines of Mg II. (The mentioned IUE observations do not resolve the h and k lines.) The KE calculations have been made by means of the LINEAR code indicated earlier. This code has been adapted to the condition appropriate to carbon-rich atmospheres and has been modified to use Voigt profiles.

One of the main characteristics of our KE calculations is that we assume the complete redistribution of photons. This analysis has been improved in studies considering partial redistribution. For our exploratory purposes, however, the assumption of the complete redistribution will be sufficient for the study of the core line formation. Only the indicated resonant lines are treated explicitly in the LINEAR code. All the other permitted transitions are considered as fixed. The radiation temperatures (T_{rad}) for the photoionizations and fixed transitions are equal to T_{eff} (with a

dilution factor of 1/2) in the chromospheric layers where T_e is larger than T_{eff}. In the following deeper layers, $T_{rad} = T_e$. A fixed-level atom is used for both Mg I and Mg II atoms. A solar Mg abundance is used.

A strong absorption Mg I line at 2852.1 A is observed in many late-type stars. (This can be seen, for instance, in the spectrum of the M3 III star, η Gem, in Johnson and O'Brien (1983).) This line, however, appears to be absent or weak in the spectra of the N carbon stars observed by Johnson and O'Brien. Normally, a strong absorption should be produced by the cooler photospheres of these stars, and this is not observed. Instead, a small emission feature appears at this wavelength in all the observed stars. Is this feature an indication of a "filling-in" process? Can an emission in the chromosphere produce this filling-in? All the Mg I lines obtained with these simple models are absorption profiles which show no sign of a central emission feature because of the strong photoionizing control of the line-source function.

An alternative filling-in process has been suggested by Johnson and O'Brien (1983) in which a large shell of gas could exist above this chromosphere. This shell must be sufficiently cool for Mg to be neutral and large enough to emit Mg I. The low-lying emission lines of Ti I, V I, and Zr I found by Gilra (1976) in the carbon star, UU Aur, could be formed in even larger shells because of their lower abundances. Scattering processes may also produce those emissions.

Figure 8-4 shows the resulting theoretical profiles of the resonance line of Mg II at λ2798 for the 3000/2.0/1.02 model. In both cases (hot and cold chromospheres), the line appears in emission with a central reversal. The shapes of these profiles are more or less typical of those found in late-type stars. One characteristic of this line is to be optically very thick, beginning to get thin only on the very top of the chromosphere. This line is, in all cases, formed at layers higher in the chromosphere than the Mg I line. The Mg II lines are much more controlled by collisions, indicating that very low radiation is available to photoionize from these two levels of the transition. The respective continua are at λ824 and λ1169, whereas those for Mg I are λ1621 and λ3756. For a general discussion on collisional and photoionization control processes, see Jefferies (1968) and Athay (1972).

The effects of the microturbulent velocities increasing outward are shown in Figure 8-5. The presented profiles are calculated for the same model 3000/2.0/1.02, both with and without microturbulence. The global effect of the velocity field is to broaden the line and shift the emission features, forming a broader reversal. More or less the same qualitative behavior has been found by Basri (1980) by means of a partial redistribution analysis. These turbulent effects are important in the detailed analyses of supergiants, which have much broader emission cores than those of dwarfs or giants.

The Avrett-Johnson Model. Apart from the Mg I and Mg II characteristics discussed above, any chromospheric model calculation of a warm N carbon star should take into account other important observational facts that act as constraints in the modeling construction. These are: (1) the presence of the emission line of C II at 2325 Å, (2) the notorious absence of the hydrogen Balmer lines (Yamashita, 1972, 1975), and (3) the reversal in the Ca II H and K lines observed in R stars (Richer, 1975) but not in N stars.

Avrett and Johnson (1984) recently constructed semiempirical chromospheres to fit these observational constraints (with the exception of the Ca II lines). The chromospheric model of an N star should be sufficiently cool to produce a low number density of the level 2 of hydrogen (n_2) to prevent the production of an Hα feature and should, at the same time, be sufficiently hot to produce Mg II and C II line emissions.

Their calculations are much more complete than the linear chromospheres calculated in the preceding subsections. They solved the

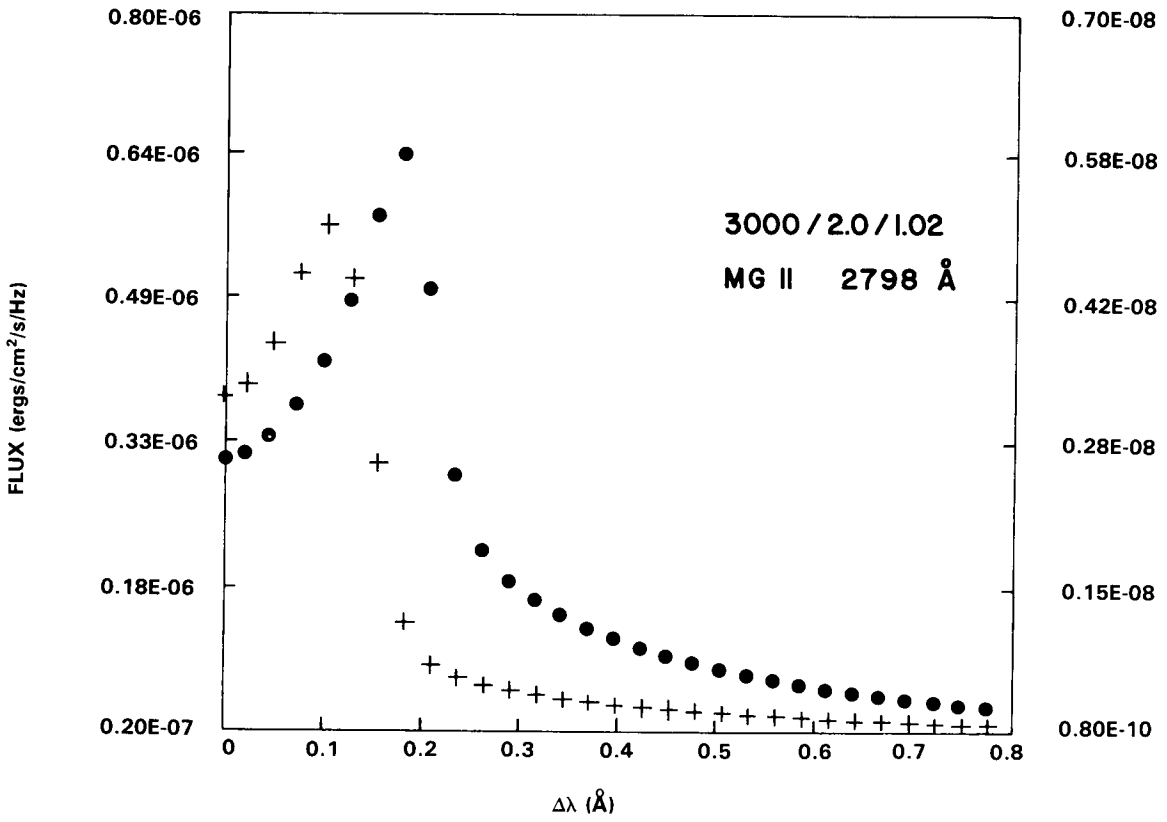

Figure 8-4. Computed profiles of the core of the resonant line of Mg II λ2798 for the model 3000/0.0/1.05. The points correspond to the hot chromosphere (flux scale on the left), and the crosses correspond to the cold chromosphere (flux scale on the right).

hydrostatic equilibria together with the KE of various elements such as H, H^-, H_2, Mg I, Mg II, C I, and C II and considered partial redistribution in the calculation of the Mg II line. The radiation temperatures used in their calculations (between 2200 and 2500 K) are smaller than those of the linear models of the subsection *Chromospheres of Carbon Stars* which have lower electron densities.

The resulting models 1 and 2 are presented in Figure 8-6, taken from the work of Avrett and Johnson (1984). The cool model 1 fills the condition of not producing the H feature; it seems, nevertheless, to be too cool to produce sufficient Mg II emission to fit the observed one. A negligible C II line is produced with this model. The hotter model 2 is also not convenient because it contains sufficient n_2 to produce an emission or absorption Hα feature, depending on whether the source function is larger or smaller than B.

In conclusion, both simple linear models and more sophisticated ones produce emission lines of Mg II. However, it is not clear whether future models will produce a C II emission feature or will maintain the H condition. (Avrett and Johnson (1984) are presently investigating hotter lower chromospheric models.) Two possible states appear to solve this problem: a high carbon abundance or a hydrogen underabundance.

Radiative Cooling and Energetic Balance. Several studies have recently appeared in the literature which treat the important problem of

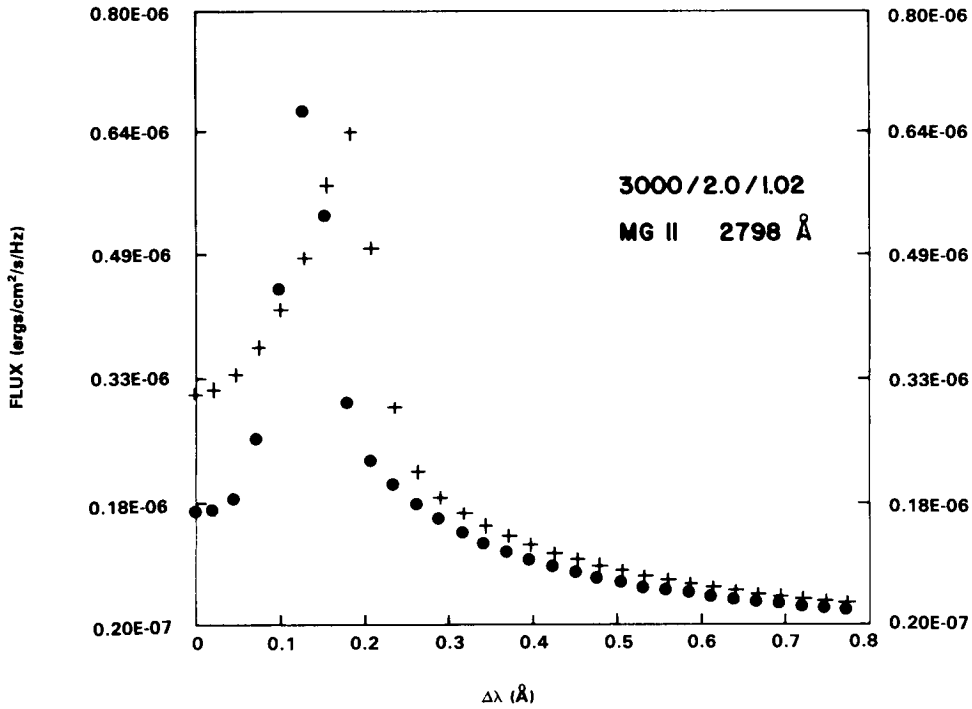

Figure 8-5. Theoretical profiles of the Mg II line for the hot model, 3000/2.0/1.02, with (crosses) and without (points) microturbulence.

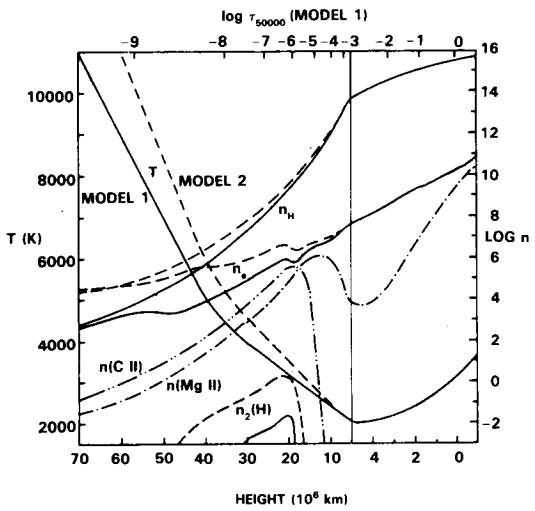

Figure 8-6. Temperature as a function of height (measured above $\tau_{5000} = 1$) for two chromospheric models and the corresponding values of the total hydrogen density, the electron density, and the level 2 hydrogen density. The τ_{5000} scale and the Mg II and C II number density for model 1 are also shown (from Avrett and Johnson, 1984).

the energetic balance in the atmospheres of the Sun and late-type stars (Linsky, 1980, 1981; Avrett, 1980). Two main processes exist in stellar atmospheres that maintain a temperature structure in equilibrium. These are the cooling and heating by radiative processes and the heating by nonradiative mechanisms. To obtain the net radiative contribution of each chemical element, the cooling and heating must be calculated for all the important bound-bound and bound-free transitions. In the chromosphere, a net radiative cooling flux results. This net cooling is a direct measure of the nonradiative (mechanical or magnetic) heating required to produce the chromosphere. In late-type giants, the lines of Ca II and Mg II are the main contribution to the net cooling, followed by H and H^-. As we go from the Sun to cooler giants, there is a growing importance of Mg II as a net cooler agent in the higher layers of the chromosphere.

For a transition between levels u (upper) and l (lower), the radiative cooling rate is (Vernazza et al., 1981):

$$\Phi'_{ul} = h\nu \, [n_u \, (A_{ul} + B_{ul} \int \Phi_\nu \, J_\nu \, d\nu) - n_l B_{lu} \int \Phi_\nu \, J_\nu \, d\nu] \, . \quad (8\text{-}26)$$

This expression can also be written using the net ϱ radiative bracket (Thomas, 1960). Note that the same symbol, Φ, is used for two different quantities:

$$\Phi'_{ul} = h\nu \, n_u \, A_{ul} \, \varrho \, , \quad (8\text{-}27)$$

where

$$\varrho = 1 - \frac{\int \Phi_\nu \, J_\nu \, d\nu}{S^L} \, . \quad (8\text{-}28)$$

Figure 8-7 presents the values of Φ'_{ul} for the resonant line of Mg II calculated for the models 3500/0.0/1.05 and 3000/2.0/1.02 with hot chromospheres. The cooling rates for the higher gravity model are found to be larger than those of the log g = 0.0 model. In fact, denser atmospheres are better radiators than diluted ones. If we can express Φ'_{ul} as a function of the geometrical depth, z, the net cooling rate can be known by calculating the integral, $\int \Phi' \, (z) \, dz$, for the positive values of Φ'_{ul}. The cooling rates shown here are presented for illustration purposes. Realistic values can be obtained by matching theoretical and observational integral fluxes.

Ultraviolet Spectra Variability. Systematic observations of ultraviolet spectral time variability are rare in S- and C-type cool giants (Cassatella et al., 1980, for the S-type star, X Cyg; Querci and Querci, 1985, for the N-type carbon star, TW Hor). Interpretation of the carbon star, TW Hor, appears to be very difficult because of the erratical behavior of emission lines such as those of Fe II at 3280 Å. As is the case in these carbon stars, several constraints must be taken into account in the atmospheric model of TW Hor, such as the absence of Balmer lines (either absorption or emission) and the absence of emission peaks of Ca II H and K lines. The Mg II emission lines appear to have a more or less normal behavior, indicating smaller variability. (For a discussion on the observations of TW Hor, see M. Querci, this volume.)

To understand the spectral characteristics of TW Hor, Querci and Querci (1985) analyzed a simple energetic budget which considers different types of physical mechanisms such as short-period acoustic waves, variable magnetic fields, and flare-like activity. The emergent picture that appears is that of a chromosphere with a flat temperature minimum and a gradual increase in higher layers. However, this increase of temperature is low enough to prevent emission peaks in Ca II H and K lines, but strong enough in higher layers to produce ionic emission features of the more abundant elements, Mg and Fe. Nevertheless, it is not clear how this chromospheric model will be able to prevent Balmer lines. The erratic behavior of the Fe II lines is, however, the most difficult aspect to understand. A variable Lα flux which induces variable Fe II emission lines (Furenlid, 1984) will not be an appropriate mechanism here because of the atypical characteristics of H in these stars. Querci and Querci (1985) state that the cause of this variability can be due to variable wave pulses (or variable magnetic field) in the chromosphere which is heated by short-period acoustic waves (Schmitz and Ulmschneider, 1981). The Mira S-type variable, X Cyg, observed by Cassatella et al. (1980) has been qualitatively interpreted using the dynamical shock-wave model of Hill and Willson (1979). (See the section *Radial Pulsation Modes.*)

SHOCK-WAVE GAS DYNAMICS AND PULSATIONAL THEORY

The preceding sections of this chapter discussed stellar photospheres and chromospheres as stationary components of static

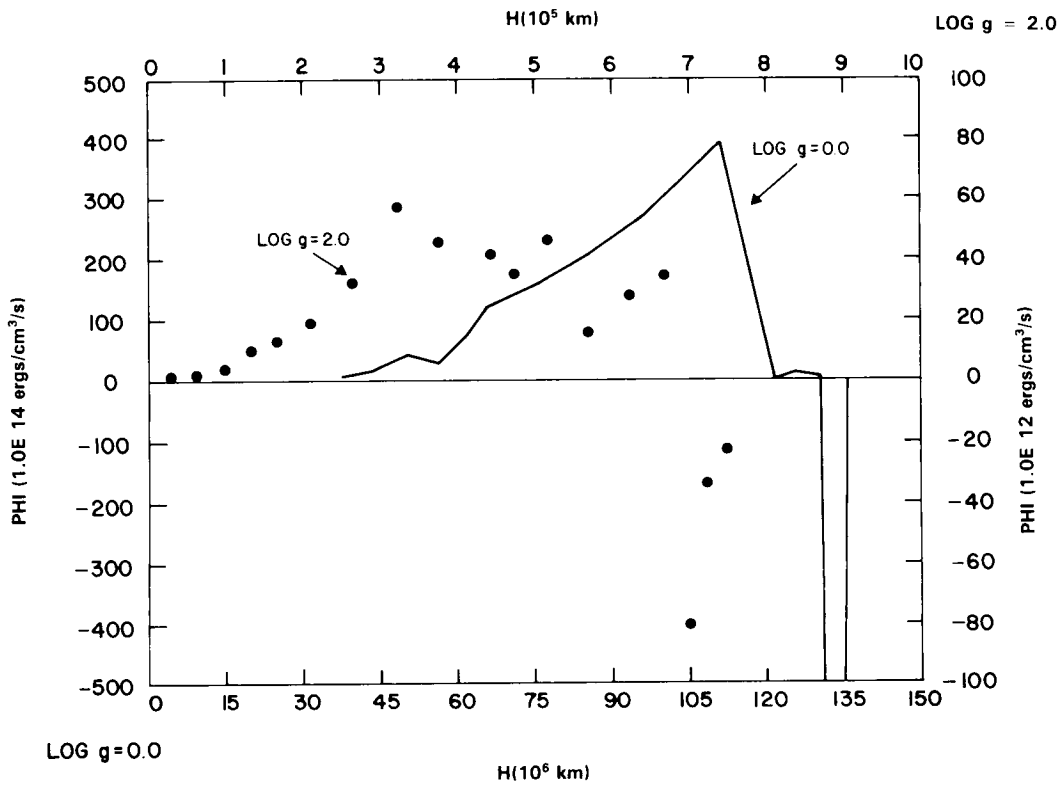

Figure 8-7. Cooling radiative functions Φ' for the Mg II line. Only the positive values contribute to the cooling. The solid line represents the hot chromosphere of the log g = 0.0 model. (The corresponding scales are on the left and on the bottom of the figure.) The points represent the hot chromosphere of the log g = 2.0 model. (The corresponding scales are on the top and right of the figure.) The top of the chromosphere is on the left.

atmospheres of single stars. However, some M and C late-type giants, as the long-period variables (Mira variables), present a complex time variability of their line spectra which requires an appropriate dynamical scenario for interpretation. Progressive shock waves are probably the principal physical mechanism that can explain this complex behavior. These shock-wave models are described by M. Querci (this volume), who focuses mainly on the observational aspects. Here we will put more emphasis on some of the basic theoretical aspects related to dynamical effects on the atmospheric structure and pulsational characteristics.

First, we will present a short discussion on the principal physical basis of the classical theory of shock waves in order to analyze the current research on this field.

Elementary Shock-Wave Theory

Gas dynamics is characterized by quantities such as velocity (v), pressure (P), density (ϱ), etc. which generally vary continuously. However, discontinuities of these quantities, which will represent shock waves, can exist. These discontinuities can move with different velocities of the gas flow itself and can be crossed by this flow of gas particles in their motion. If we consider a fixed coordinate system in which we define v_n as the gas velocity normal to the surface and v_s as the velocity of the discontinuity (shock wave), $u = v_n - v_s$ will be the velocity

of the gas relative to the discontinuity. Let us call gas 1 the one into which the discontinuity moves (preshock) and 2 the gas which follows the discontinuity (postshock). The respective velocities will be u_1 and u_2.

One of the most important theoretical tools that enable us to treat shock waves is the fact that the laws of mass, momentum, and energy conservation can be applied to those discontinuity regions. Applying these laws (see, for instance, Zeldovich and Raizer, 1966), we have the following respective equations:

$$\varrho_1 u_1 = \varrho_2 u_2 , \tag{8-29}$$

$$P_1 + \varrho_1 u_1^2 = P_2 + \varrho_2 u_2^2 , \tag{8-30}$$

$$\epsilon_1 + \frac{P_1}{\varrho_1} + \frac{u_1^2}{2} = \epsilon_2 + \frac{P_2}{\varrho_2} + \frac{u_2^2}{2} , \tag{8-31}$$

where P, ϱ, and ϵ are the pressure, density, and internal energy, respectively. Equation (8-29) reflects the existence of a continuous mass flux crossing a "zero-mass" discontinuity. Equation (8-30) represents the existence of the continuous momentum flux, meaning that the force exerted by the gases on each other across the discontinuity must be equal. If no external energy sources are considered, Equation (8-31) means that the internal energy, ϵ, of a given element is the result of the compressive work done on the element by the surrounding medium.

The Hugoniot Relations. A new important relation can be obtained from the conservation laws. Introducing the specific volumes, $V_1 = 1/\varrho_1$ and $V_2 = 1/\varrho_2$, we obtain from Equation (8-29):

$$\varrho_1 u_1 = \varrho_2 u_2 = J \tag{8-32}$$

that $u_1 = JV_1$ and $u_2 = JV_2$. Substituting in Equation (8-30), we obtain

$$J^2 = \frac{P_2 - P_1}{V_1 - V_2} . \tag{8-33}$$

Since J^2 is positive, two possibilities may arise: $P_2 > P_1$, $V_1 > V_2$ or $P_2 < P_1$, $V_1 < V_2$. In realistic shock waves, only the first case may actually occur. This corresponds to stable compression waves that result in an increase of entropy (Zeldovich and Raizer, 1966).

We can write Equation (8-31) in the following form:

$$\epsilon_1 + P_1 V_1 + \frac{1}{2} J^2 V_1^2 = \epsilon_2 + P_2 V_2 + \frac{1}{2} J^2 V_2^2 . \tag{8-34}$$

Replacing J^2 from Equation (8-33), we find finally:

$$\epsilon_2 - \epsilon_1 = \frac{1}{2} (P_1 + P_2)(V_1 - V_2) . \tag{8-35}$$

This relation is known as the *shock adiabatic* or *Hugoniot relation*. Graphically, this relation is represented in a PV-plane by Figure 8-8. An important conclusion can be obtained simply from this relation. First, we will determine the physical behavior of weak shock waves for small values of $P_2 - P_1$ and $V_2 - V_1$. Equation (8-33) can be written in first approximation as:

$$J^2 = - \frac{\partial P}{\partial V} . \tag{8-36}$$

The velocities u_1 and u_2 being equal in the same approximation, we have:

$$u_1 = u_2 = u = JV . \tag{8-37}$$

With Equation (8-36), we obtain:

$$u = \left[- V^2 \left(\frac{\partial P}{\partial V} \right) \right]^{1/2} = \left(\frac{\partial P}{\partial \varrho} \right)^{1/2} , \tag{8-38}$$

which is the velocity of sound C for that medium. We can conclude that, in the first approximation, the propagation velocity of a weak shock is equal to the velocity of sound,

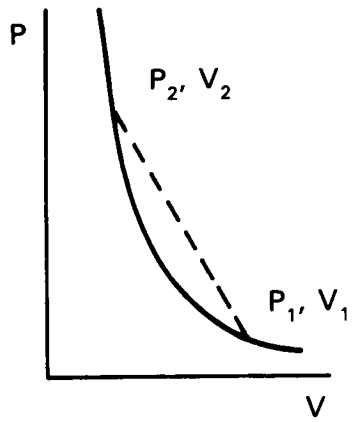

Figure 8-8. Graphical representation of the Hugoniot curve in a pressure-specific volume plane.

or in other words, the weak shock is a small perturbation that is approximately the same as a compression sound wave. Because real shock waves are compression waves, we must have $P_2 \quad P_1$. The point, 1 (P_1, V_1), must lie below the point, 2 (P_2, V_2), in Figure 8-8. Chord 12 has a slope J^2 larger than the tangent to the adiabatic at point 1:

$$J^2 > - \frac{\partial P}{\partial V_1} \tag{8-39}$$

Multiplying both sides by V_1^2, we have:

$$\begin{aligned} J^2 V_1^2 = u_1^2 &> V_1^2 \left(\frac{\partial P}{\partial V_1} \right) \\ &= \frac{\partial P}{\partial \varrho_1} = C_1^2 \quad . \end{aligned} \tag{8-40}$$

Then,

$$u_1 > C_1 \quad . \tag{8-41}$$

The gas flows into the discontinuity with a supersonic velocity. In other words, the shock wave propagates at a supersonic velocity with respect to the undisturbed gas 1. The slope of the chord being smaller than the adiabatic tangent at point 2, we obtain in the same manner as before that:

$$u_2 < C_2 \quad . \tag{8-42}$$

This means that the gas flows out of the discontinuity with a subsonic velocity, or in other words, the shock wave propagates at a subsonic velocity with respect to the compressed gas behind it. Because of the compression, $\varrho_2 > \varrho_1$, we have by means of Equation (8-29) that $u_1 > u_2$.

Shock Waves in a Perfect Gas. If we now consider the shock waves in a perfect gas with a constant ratio of specific heat, γ, we can introduce the internal energy:

$$\epsilon = \frac{PV}{\gamma - 1} \quad , \tag{8-43}$$

into the Hugoniot relation (8-35) and obtain the following relation:

$$\frac{V_2}{V_1} = \frac{(\gamma + 1) P_1 + (\gamma - 1) P_2}{(\gamma - 1) P_1 + (\gamma + 1) P_2} \quad . \tag{8-44}$$

Also, using the state equation of a perfect gas, we obtain the ratio of temperatures of the two sides of the discontinuity to be:

$$\frac{T_2}{T_1} = \frac{P_2 (\gamma + 1) P_1 + P_2 (\gamma - 1) P_2}{P_1 (\gamma - 1) P_1 + P_1 (\gamma + 1) P_2} \quad . \tag{8-45}$$

From Equations (8-29), (8-30), and (8-44), we can obtain the velocities of propagation of the shock waves relative to the preshock and postshock gases:

$$u_1^2 = \frac{1}{2} V_1 \left\{ (\gamma - 1) P_1 + (\gamma + 1) P_2 \right\} \quad , \tag{8-46}$$

$$u_2^2 = \frac{1}{2} V_1 \left\{ (\gamma + 1) P_1 + (\gamma - 1) P_2 \right\}^2 \Big/ \left\{ (\gamma - 1) P_1 + (\gamma + 1) P_2 \right\} \tag{8-47}$$

In the case of very strong shock waves for which $P_2 \gg P_1$ and $P_2 \gg (\gamma + 1)P_1/(\gamma - 1)$, we obtain the following result from Equations (8-44), (8-45), (8-46), and (8-47):

$$\frac{V_1}{V_2} = \frac{\varrho_2}{\varrho_1} = S = \frac{\gamma + 1}{\gamma - 1} , \quad (8\text{-}48)$$

$$\frac{T_2}{T_1} = \frac{\gamma - 1}{\gamma + 1} \frac{P_2}{P_1} , \quad (8\text{-}49)$$

$$u_1 = \left[\frac{1}{2} (\gamma + 1) P_2 V_1 \right]^{1/2} , \quad (8\text{-}50)$$

$$u_2 = \left[\frac{1}{2} (\gamma - 1)^2 P_2 V_1/(\gamma + 1) \right]^{1/2} . \quad (8\text{-}51)$$

These relations have important physical implications. First, the ratio, T_2/T_1, can be as large as P_2/P_1; second, the velocities, u_1 and u_2, depend on the square root of P_2. This means that T_2 and the velocities can take very large values.

This is not the case for the density, ϱ_2. In fact, the ratio of densities S will attain a constant value, depending on the value of γ: $S = 4$ for a monoatomic gas with $\gamma = 5/3$, and $S = 6$ for a diatomic gas with $\gamma = 7/5$. If full vibration/excitation is taken into account with $\gamma = 9/7$, S will be equal to 8. This ratio can be even larger if dissociation of molecules, excitations, and ionizations of the atoms or ions are taken into account.

Shock Model Applications

Three main directions characterize the work related to shock waves in the atmospheres of late-type stars: (1) the energy balance (the influence on the thermal structure), (2) the modes of pulsation which induce the shocks, and (3) shocks as a mechanism that produces mass loss. As mentioned previously, the observational evidence of the presence of shock waves, their behavior, and the models interpreting them are presented in detail in Chapter 2 (M. Querci). Here we will mention those observational aspects related to specific points of the theoretical discussion.

The motivation of the first theoretical approaches was to explain the origin of the bright hydrogen lines. Gorbatskii (1961) made one of the first theoretical studies of the ionization and radiation of zones heated by shock waves. This study, however, did not take into account the dissociation of the H_2 molecule, which is an important cooling effect. Later, Whitney and Skalafuris (1963) studied the restricted case of the behavior of the high-temperature region between 10000 to 30000 K near the shock front in a pure hydrogen atmosphere with no density gradient in front of the shock. The effects of the dissociation of the H_2 molecule have been taken into account by Slutz (1976) in his study of the acceleration of a single isolated adiabatic (with no radiative energy losses) shock wave in a photosphere having a density gradient. This study shows that, if the shock has a large amplitude, the acceleration ends in a terminal velocity smaller than 25 km s^{-1} (this value depending on the quantity of H_2). This could imply that, for stars with an escape velocity smaller than 20 km s^{-1}, an ejection of a shell of matter is possible. However, this kind of shock, called first shock, has been shown by Wood (1979) to be an atypical shock. In fact, a typical shock would be the one moving into matter falling inward, originated by a preceding shock, or matter flowing outward in a form of cool stellar wind. In addition, the proper initial conditions must be correctly established to consider the periodical nature of the problem. A sinusoidal varying pressure which simulates the star pulsation could be this initial condition.

The intrinsic pulsation nature of cool giants or supergiant variable stars (see, for example, M. Querci, this volume) could be the source of shock waves. Even the microturbulent or macroturbulent velocities, in spite of being generally ill-determined quantities, are sometimes found to be larger than the sonic velocities and

are therefore able to produce shock waves. However, it is in the interpretation of the complex spectra of Mira variables that the most powerful evidence of the presence of shock waves is found. The work of Willson (1976) is, in this respect, the most illuminating. Without considering in detail the complex behavior, doubling, and variations of absorption and emission lines (M. Querci, this volume), we mention the existence of two types of lines. The primary lines of Mg II, Ca II, Fe, and Ti II, formed in the region behind the shock (region 2) and the secondary lines of Sc I, Mn I, and Fe I (fluorescent or pumped lines) formed in front of the shock (region 1).

The main argument of Willson (1976) is that the fluorescent lines are formed by excitation of radiation emitted by the primary lines in a region of velocity discontinuity (shock wave). Each fluorescent line has its proper primary line exciting radiation approaching or receding with a characteristic velocity difference, producing an appropriate shift. Willson was able to show that, in general, the complex spectrum of typical Mira LPV atmosphere could be interpreted by a velocity discontinuity of the order of 40 to 80 km s^{-1}, thus providing strong evidence of the existence of a shock wave. Broadly speaking, the picture is the following: a moderately strong shock with a mean velocity of near 50 km s^{-1} appears at the base of the photosphere shortly after the visual light maximum. As this shock travels outward, it thermally excites the primary lines behind the shock; these lines at their turn radiatively excite (or pump) the fluorescent lines in the regions in front of the shock.

It is important to realize that the fluorescent lines permit one to determine only a velocity discontinuity (Δv), not the actual shock-wave velocity (v_s) with respect to the center of mass of the star. Positive or negative Δv indicates whether an exciting atom is approaching or receding from the region in which the excited (pumped) lines are formed. In this way, Δv 0 will mean that the compressed region 2 is moving outward. In this region, as discussed in the section *Elementary Shock-Wave Theory*, $u_2 = v_2 - v_s$, where v_2 is the gas velocity normal to the discontinuity. From relation (8-42), we see that this difference is smaller than the speed of sound, C_2, which is less than 10 km s^{-1} for a gas at $T < 10^4$ K and a typical density of 10^{-12} gr cm^{-3}. Taking into account the limited precision of the measurements, we can say that $v_2 \approx v_s$. In that condition, the velocity u_1 (velocity of the shock with respect to region 1) is a good measure of Δv obtained by the fluorescent lines: $u_1 \approx \Delta v$. If region 1 is falling toward the star, the actual shock velocity would be smaller than Δv, $v_s = v_2 = \Delta v - v_1$. On the contrary, if the material is flowing outward, the velocity of the compressed region will be larger, $v_s \approx v_2 = \Delta v + v_1$.

Influences on the Thermal Structure. The existence of a supplementary kinetical energy due to shocks produces an extension of the entire scale of the atmosphere of a late-type giant or supergiant star. This extension can be a factor 10 greater than the nonshocked atmosphere. For example, for a star with a radius equal to 10^{10} cm, this scale is similar to the stellar radius (Willson, 1976). The shock waves must then be considered as spherical shock waves which produce observable effects at greater distances from the stellar surface. In fact, shocks can persist for more than a period, and the product of the period and the shock velocity is of the order of the stellar radius.

We also expect to find structural changes in the distribution of temperature and density. However, these changes are not clearly determined at the present time because of the absence of a detailed calculation of the coupled interaction of the structure parameters and the detailed study of the shocks. A comparison between plane-parallel and the more realistic spherical isothermal atmospheres can be found in Willson (1982). The main theoretical approaches have been made using two different models: adiabatic (Wood, 1979) and isothermal (Willson and Pierce, 1982). The isothermal condition is expected to be satisfied in the lower

dense regions of the photosphere in which some absorption lines can be formed. Due to the higher density, any shock-heated material can cool more efficiently. This cooling is then produced in a small distance compared to the entire scale of the atmosphere. The isothermal condition is less valid in the outer less dense regions. We then expect a progressive change toward the adiabatic condition.

Using a pure adiabatic model, Wood (1979) found a resultant decreasing temperature distribution corresponding to a mean heating of the order of 5000 K in relation to an initial hydrostatic atmosphere. However, this adiabatic model produces an unrealistic high mass-loss rate. Using the isothermal approximation, Willson and Pierce (1982) found, in an atmosphere which suffers repeated shock passages, that the minimum temperature attained between shocks is an increasing outward function, contrary to the adiabatic case mentioned before. Due to the failure of the isothermal approximation at densities lower than $\log \varrho = -15$ (corresponding to a radius larger than $900\, R_\odot$), these authors can no longer describe the gas in the outer regions by a single temperature. In this picture we do not have a clear idea of the height at which the shocked model will attain a temperature low enough to allow the formation of dust grains. When dust grains are formed, they will produce heating by gas/grain collisions. At the same time, opposite cooling processes will appear such as rotational cooling of molecules or a simple adiabatic expansion. A recent work by Tielens (1983) has considered all these factors in a study of the flows of Mira variables driven by radiation pressure on dust grains. Tielens especially considered the direct coupling of the cooling of the gas with the velocity gradients in a two-component fluid composed by dust and gas interacting by collisions. This study is related to the existence of a stationary layer located between 5 and 10 R_* from the star, in which matter can return to the star or be pushed outward. The existence of this layer at 800 K at 10 R_* from which the maser features of SiO could originate, is proposed by Hinkle et al. (1982) and Hinkle (1983).

Detailed Structure of Shock Waves. Some studies of the detailed physical parts of stellar shocks appeared recently in the literature (Gillet and Lafon, 1983, 1984, in a strictly theoretical point of view; Fox et al., 1984, combining theory and observations). (See also the subsection *Shock-Wave Gas Dynamics of Balmer Emission Lines.*) A complete detailed analysis of the shock regions would be quite difficult, especially when the real finite shock front is considered, in which very large gradients of the physical variables have to be taken into account. Appropriate mathematical methods will then be necessary. Perhaps one promising method for future studies is the "Adaptive-Mesh Radiation Hydrodynamics" (Winkler et al., 1984). Here, an adaptive coordinate system, fixed neither to the fluid nor to the laboratory, is free to follow the evolution of the flow and the radiation field. The importance of this method is that, although the observed quantities are measured, for instance, in a comoving frame of the fluid, the radiation transport equation can be written in this adaptive frame which can move with arbitrarily high velocities. Large gradients such as shock fronts can then be treated.

As mentioned in the subsection *Shock Waves in a Perfect Gas*, the ratio $S = \varrho_2/\varrho_1$ can change if excitation and ionization are taken into account. It can be demonstrated that the increase of S for a given T depends on molecular dissociation and the internal energy of the particles (e.g., ionization) (Zeldovich and Raizer, 1966). Values larger than $S = 10$ can be obtained for high degrees of dissociation and ionization. In a medium composed of a mixture of gases, we expect to find a variable behavior of S as the strength of the shock increases.

In a medium formed by pure H, Gillet and Lafon (1984) analyze the precursor region (e.g., the immediate preshock region), putting emphasis on the importance of molecules in the weakening of the shock. For this, they considered the physical nonlinear relation between the precursor and the postshock region. In fact, before being affected by the advancing front,

the precursor is already influenced by the radiation coming from the hot postshock region. This radiation photodissociates the molecules and photoionizes the medium, producing a radiative cooling of the postshock region. This cooling is further accentuated by the thermal dissociation of molecules that cross the front.

Pulsation Theory

Radial pulsations are clearly seen in a large part of luminous M and C cool stars (see M. Querci, this volume). The aim of the theoretical research on the pulsation theory on these stars has been to answer the following fundamental and difficult questions: (1) Which is the pulsation mode? (2) Is pulsation an effective mass-loss mechanism? To answer these questions, linear (and nonlinear) adiabatic (and nonadiabatic) pulsation models have been developed in recent years. However, even with the great effort of some authors, no definite answers to these questions have been given.

Pulsations are produced in the large diluted envelopes of the stars in which the high luminosity determined by the core mass is being transported essentially by a convective process. The luminosity in these late-type stars can be so high that a net positive energy produces a dynamical instability. The pulsation provokes shock waves that locally heat and probably extend the atmosphere. This pulsational instability can relax into a steady regular pulsation such as those observed in LPV stars. However, the pulsations can also be transformed into strong relaxing oscillations in which mass loss can occur (Tuchman et al., 1978). Nevertheless, the success of this mechanism in interpreting real variable stars unfortunately depends on a badly known time-dependent convection theory. Another important theoretical input is the necessity to introduce realistic surface boundary conditions. Wood (1980) clearly shows these necessities when he discusses the uncertain results concerning the pulsational instabilities mentioned above and those of Wood (1979) and Willson and Hill (1979). In these models, not only convection is the weakest point, but also the mass loss produced. In fact, only few external zones are ejected, and the consideration of a proper external boundary, such as circumstellar material, could inhibit this mass loss. A general discussion on these aspects can be found in Wood (1982). More details concerning mass loss can be seen in Goldberg (this volume).

Nonradial Pulsations. Although pulsation has been discussed as a radial oscillation, there is a possibility of the existence of nonradial oscillations as supplementary energy-transporting mechanisms other than convection. These oscillations have been explored by linear nonadiabatic calculations in late-type models by Ando (1976). Later, Smith (1980) considered the possibility that these nonradial oscillations could be the source of what is commonly called "macroturbulence." The predicted amplitudes of this "late-type star seismology" are nevertheless very small, probably a few tenths of ms^{-1}. They would therefore be very difficult to detect. Recent observations in this direction are not yet conclusive (Smith, 1983, in α Tau and α Boo; Moon et al., 1983, in an M-S giant, ϵ Oct). Other promising candidates could be the following M semiregular giants which show short-period variations, particularly of the spectral region around the Ca I λ4227 absorption feature: R Crt (Livi and Bergmann, 1982) and L_2 Pup (Gómez Balboa and de la Reza, 1985).

Radial Pulsation Modes. One of the fundamental relations of radial pulsational stellar theory is the period-density relation (see for instance, Cox, 1980) which introduces the pulsation constant, Q, in the form:

$$Q = P(\varrho/\varrho_\odot)^{1/2} = P(M/M_\odot)^{1/2}\,(R/R_\odot)^{-3/2}\,. \qquad (8\text{-}52)$$

However, as has been shown in linear nonadiabatic models (Fox and Wood, 1982), Q is not a constant for any of the three lower order radial pulsation modes (fundamental, first and second overtone modes). Figure 8-9

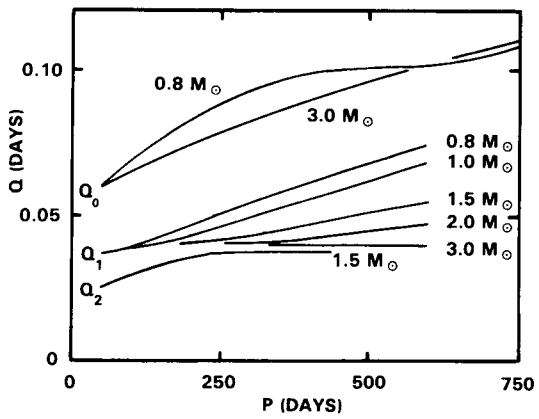

Figure 8-9. Q values for the three lowest order radial pulsation modes plotted against period (from Wood, 1982).

presents their corresponding values of Q_0, Q_1, and Q_2 against the first overtone period. If molecular opacity is introduced, Q_0 will be reduced. On the contrary, Q_1 will be somewhat larger. Another result of Fox and Wood is that, for high-luminosity stars, the nonadiabatic fundamental period, P_0, is shorter than the adiabatic, P_0. This has an important consequence because the adiabatic dynamical instabilities produced by large periods (Tuchman et al., 1978) disappear when nonadiabatic effects are included. In this linear nonadiabatic regime, the fundamental period, P_0, behaves as $P_0 \alpha R^2$ rather than $P \alpha R^{3/2}$ of the classical relation (8-52). An approximate simple relation can be found for Q_0 between definite values of M and P. No simple relation, however, can be found for the first overtone period, P, which behaves as $R^{3/2}$ for higher mass and as $R^{5/2}$ for lower mass. These results are found for typical galactic-disk long-period and semiregular variables. The L–M–R relations change when massive disk supergiants (up to 25 $M_\odot$) or other populations with different metallicities are considered.

Linear and nonlinear nonadiabatic pulsation models have also been investigated by Ostlie et al. (1982) in view of applications to typical galactic Mira stars. They obtain P–M–R relations for fundamental and first overtone pulsations, examining in particular the effect of a turbulence pressure. In the linear case, pressure effects appear to be important for the fundamental mode and lower mass. In the nonlinear models, turbulence amplifies the nonadiabatic effects.

How do Mira stars pulsate? This is a controversial subject, and no definite answers have been given. Looking back to the past, Kamijo (1963a, 1963b) concluded that Miras do not pulsate in the fundamental mode, but rather in higher modes with shorter periods. Later, the research has been based on the possibility of finding stable pulsational adiabatic static models (Keeley, 1970; Wood, 1974, 1975). The introduction of more realistic nonadiabatic models has introduced stable models which can be applied to massive LPV supergiants and pulsating carbon giant stars. These stars show secondary periods with $P \sim 2000$ to 7000 days (Leung and Stothers, 1977), which are approximately 7 times the typical primary periods of 300 to 700 days. Fox and Wood (1982) found several supergiant models in which $P_0/P_1 \sim 7$, indicating that the primary period is produced by excitation of the first overtone and the secondary period of the fundamental mode.

Let us now discuss the arguments supporting the fundamental mode pulsation of Miras. These are based on a dynamical model of shock waves (Willson and Hill, 1979; Hill and Willson, 1979; Willson et al., 1982). A general discussion can be found in Willson (1982). In particular, Hill and Willson (1979) developed a dynamical model, and in their calculations, they used the spherical symmetry and isothermality assumptions. Their model is characterized by the existence of two shocks. One lower shock emerges, with large amplitude, at the photosphere and lasts about a period. With the next period, another shock appears; two shocks can then be present: one stronger and lower and another weaker and higher. This lower shock is formed near the piston by the impact of the infalling large volume of rarefied preshock material with the rising material near the

C-6

photosphere. Because rarefied matter is falling and dense compressed material is rising, no net inward or outward motion is produced in this model.

In this model, the lower shock gives rise to the hydrogen emission lines in the postshock region, whereas the passage of the weaker upper shock model affects the absorption lines. The emission and absorption velocities then show the velocity variation across the lower and upper shock velocities, respectively.

In both these shocks, we can define $\Delta v = v_2 - v_1$, where v_1 and v_2 are the velocities defined in the section *Elementary Shock-Wave Theory*. Considering the relation (8-29), we obtain:

$$-v_2 = \frac{\Delta v}{S-1} \quad , \tag{8-53}$$

$$-v_1 = \left(\frac{S}{S-1}\right) \Delta v \quad . \tag{8-54}$$

Because $u_2 = v_2 - v_s$, where v_s is the shock velocity, it can be written as:

$$v_s = \frac{dr_s}{dt} = (1+q)\, v_2 \quad , \tag{8-55}$$

where

$$q = \frac{\Delta v / v_2}{S-1} \quad . \tag{8-56}$$

For a strong shock (higher S), $v_s \approx v_2$.

One important consequence of the model of Hill and Willson (1979) is that the ratio defined by $\beta = v_2/v_e$ is nearly constant, and equal to 0.2. v_e is the escape velocity $(2\ GM/r_o)^{1/2}$, where r_o is the radial distance of the lower shock. The value and behavior of β characterize the dynamical aspect of the model and is the basis of the interpretation of the observational results. In that case,

$$v_2(r) = \beta\, v_e(r) = v_2(r_o)\,(r/r_o)^{1/2} \quad . \tag{8-57}$$

For constant values of β and q, the solutions of Equations (8-55) and (8-57) give:

$$v_2\,(t=P) = v_2\,(t=o) \left[1 + \frac{3}{2}\,(1+q)\,\frac{v_2\,(o)\,P}{r\,(o)}\right]^{-1/3} \tag{8-58}$$

Hill and Willson (1979) place, in an M–R diagram (see their Figures 10 and 11), the values of constant velocity $v_2(o)$ and $v_2\,(P)$ for the stars R Leo and O Cet. It is possible to find a region in this diagram that is best satisfied by the observational data. Probable masses and radii are then obtained for R Leo (M = 1.8 - 4.0 $M_\odot$, R = 1.7 - 2.5 × 10^{13} cm) and for Mira ($M \approx 0.8$ - 1.5 $M_\odot$, $R \approx$ 1.3 - 2.0 × 10^{13} cm).

Lines of constant Q values also allow one to establish the best possible pulsation modes between Q = 0.1 (fundamental mode) and Q = 0.04 (overtone mode). Both values seem a priori satisfactory; however, considering supplementary data on masses and radii, Hill and Willson (1979) preferred the fundamental mode for both stars.

The work of Hill and Willson (1979) has been criticized by Wood (1980, 1982). As mentioned previously, considerable controversy exists about this subject. Wood (1975, 1980) favors the first overtone mode. Wood derived larger radii (smaller Q) than those of Hill and Willson. Nevertheless, the principal arguments of Wood concern the dynamical and kinematical interpretations of the measured shock velocities in LPV. On the dynamical aspect, Wood (1979) found that, if a radial temperature gradient is introduced, the ratio β is no longer constant, being 0.24 for a lower shock and 0.11 for an upper shock. The other point of discussion concerns the possibility of measuring the values of the postshock velocity of the upper shock. Wood (1980, 1982) showed that, if the upper shock velocity can be measured, its low accuracy will severely compromise the results. In fact, for a dynamical shock-wave model, Q is very sensitive to the

velocity values because $Q \alpha (v_{lower}/v_{upper})^3$, and an uncertainty of ± 1 km s^{-1} will introduce an error in the determination of Q of the order of ± 0.1.

In conclusion, we can say that appropriate surface boundary conditions will help future studies. These conditions will probably affect primarily the overtone pulsations, which are more surface phenomena than those of the fundamental mode. A new approach, based on the detailed shock evolution of the Balmer emission lines, is now beginning to be explored.

Shock-Wave Gas Dynamics of Balmer Emission Lines. The observed behavior of the Balmer emission lines in different phases of Mira variables has been known since the pioneer works of Merrill (1945) and Joy (1947), but not until now have careful high spectral resolution observations of these lines been made in order to study the pulsation properties (Fox et al., 1984). A qualitative study of the dynamical evolution of Hα in the star, o Cet, has also appeared recently (Gillet et al., 1983), in which the variations of the Hα emission profile is interpreted as a spherical shock wave propagating outward from the photosphere. The shock leaves the photosphere when Hα emission appears for the first time in the cycle. Because of the occultation by the photosphere, the observer sees only the advancing part (detecting a blue-shifted emission). The emission profile appears to be mutilated by absorptions of an external molecular region. This mutilation diminishes as the shock leaves the molecular region. At that moment, the shock is quite far from the photosphere, and the observer is able to see the receding part of the always-outgoing shock, now producing a red-shifted emission. The atmosphere is then crossed from the luminosity maximum to the minimum by a single strong spherical shock wave which produces the emission lines in the hot postshock region. However, observed evidence of a second supersonic infalling shock in the same star has been detected by Ferlet and Gillet (1984) by means of an inverse P Cygni profile of Ti I. This infalling shock could be the return of nonejected upward-accelerated matter.

Fox et al. (1984) published a series of high-resolution spectral observations of the Balmer lines Hγ, Hδ, Hζ, and Hη of nine Mira stars during half cycle around maximum phase. Observations of the thermal excited line, Mg I λ4571, and the pumped line, Fe I λ4202 (pumped by the Mg II resonance line at λ2795), were also made. The Balmer emission lines present a full base width of near 80 km s^{-1} which decreases at later phases. Hδ seems to be the most indicated line for the study of evolution of emission regions because it is the least affected by superposed absorptions.

A detailed shock model to be applied to these observations is in progress (Fox and Wood, 1985). However, in advance of the presentation of this detailed model, a schematic simple shock is presented by Fox et al., (1984). This shock is shown in Figure 8-10. The precursor is formed by H and He at $T \sim 2500$ K, with an infalling velocity of 20 km s^{-1}. The hot postshock region is at $T = 34500$ K. It is in this region that the broad emission lines are formed by an important Balmer line scattering. In fact, the broadening temperature of the lines indicate temperatures of the order of 30000 K. The velocities shown in Figure 8-10 agree with those obtained from high-infrared spectroscopy of CO lines (Hinkle et al., 1984). In the shock model of Fox and Wood (1985), the far side of the outgoing shock does not contribute to the observed Balmer emission because of the total absorption of the inward Balmer radiation. This is contrary to the Hα interpretation of Gillet et al. (1983) mentioned previously. The metallic lines observed are very important in that they permit the Balmer emission variations in the cycle to be related to the velocities obtained from these metallic lines. This relation suggests a slowing down of the shock with phase. A further study is necessary to determine where the Mg I and Fe I lines mentioned are formed. Are they formed in the precursor or in the postshock region? The detailed model

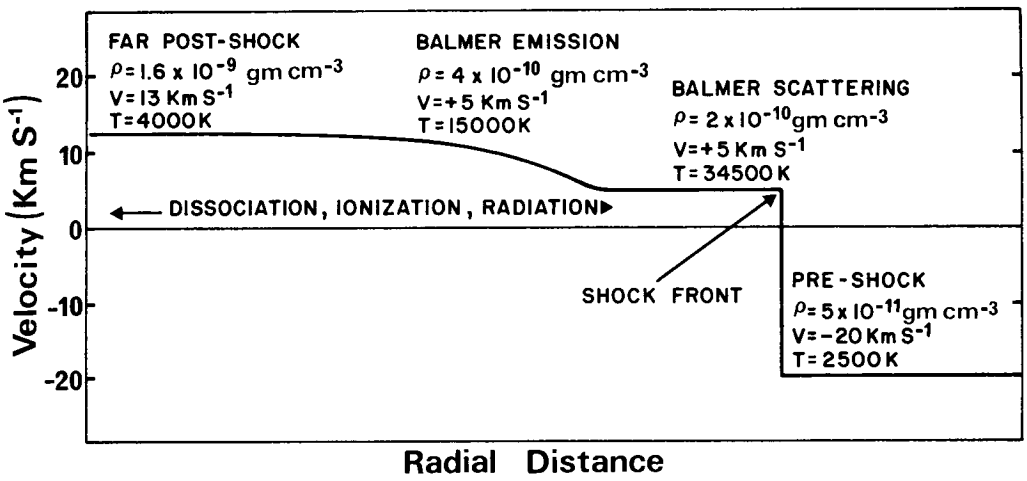

Figure 8-10. A schematic diagram of shock structure in a typical Mira variable near-maximum light. Velocities are in the rest frame of the star (from Fox et al., 1984).

of Fox and Wood will possibly give the answers and may give new information concerning the pulsation modes of the Mira stars investigated.

REFERENCES

Ando, H. 1976, *Pub. Astron. Soc. Japan*, **28**, 517.

Athay, R.G. 1972, *Radiation Transport in Spectral Lines* (Dordrecht: Reidel).

Athay, R.G. 1981, *Astrophys. J.*, **250**, 709.

Athay, R.G., and Skumanich, A. 1967, *Ann. Astrophys.* **30**, 669.

Auer, L. 1973, *Astrophys. J.* **180**, 469.

Auer, L.H., Heasley, J.R., and Milkey, R.W. 1972, *Kitt Peak Obs. Contrib. 555.*

Auman, J.R., and Woodrow, J.E.J. 1975, *Astrophys. J.* **197**, 163.

Avrett, E.H. 1980, in *Proc. Nato Adv. Inst., Solar Phenomena in Stars and Stellar Systems*, ed. A.K. Bonnet-Duppree (Bonas).

Avrett, E.H. 1985, to appear in *Proc. Sac. Peak Workshop, Chromospheric Diagnosis and Modeling*, ed. B. Lites.

Avrett, E.H., and Johnson, H.R. 1984, in *Proc. Third Cambridge Workshop, Cool Stars, Stellar Systems, and the Sun*, ed. S.L. Baliunas and L. Hartmann (Berlin-Heidelberg, New York, Tokyo: Springer-Verlag).

Avrett, E.H., and Loeser, R. 1969, *Smith. Astrophys. Obs., Special Report. 303.*

Avrett, E.H., and Loeser, R. 1983, in *Methods in Radiative Transfer*, ed. W. Kalkofen (Cambridge: Cambridge Univ. Press), p. 341.

Ayres, T.R. 1981, *Astrophys. J.*, **244**, 1064.

Ayres, T.R. 1985, to appear in *Proc. Sac. Peak Workshop, Chromospheric Diagnosis and Modeling*, ed. B. Lites.

Ayres, T.R., Moos, H.W., and Linsky, J.L. 1981, *Astrophys. J. (Letters)*, **248**. L137.

Baliunas, S. 1983, *Pub. Astron. Soc. Pacific*, **95**, 532.

Basri, G.S. 1980, *Astrophys. J.*, **242**, 1133.

Basri, G.S., Linsky, J.L., and Eriksson, K. 1981, *Astrophys. J.*, **251**, 162.

Boesgaard, A.M. 1979, *Astrophys. J.*, **232**, 485.

Boesgaard, A.M. 1981, *Astrophys. J.*, **251**, 564.

Boesgaard, A.M., and Magnan, C. 1975, *Astrophys. J.*, **198**, 369.

Brown, A., and Carpenter, K.G. 1985, JILA, University of Colorado, preprint.

Carbon, D.F., Milkey, R.W., and Heasley, J.N. 1976, *Astrophys. J..*, **207**, 253.

Carpenter, K.G., Brown, A., and Stencel, R.E. 1985, *Astrophys. J.*, **289**, 676.

Cassatella, A., Heck, A., Querci, F., Querci, M., and Stickland, D.J. 1980, in *Proc. Second European IUE Conference*, ESA SP-157.

Cox, J.P. 1980, *Theory of Stellar Pulsation* (Princeton: Princeton Univ. Press).

de la Reza, R., and Querci, F. 1978, *Astron. Astophys.*, **67**, 7.

Draine, B.T. 1981, in *Physical Processes in Red Giants*, ed. I. Iben and A. Renzini (Dordrecht: Reidel), p. 317.

Drake, S.A. 1984, *Progress in Stellar Spectral Line Formation Theory* (Trieste), ed. J.E. Beckman and L. Crivellari (Dordrecht: Reidel).

Drake, S.A., and Linsky, J.L. 1983, *Astrophys. J.*, **273**, 299.

Dyck, H.M., and Johnson, H.R. 1969, *Astrophys. J.*, **156**, 389.

Eaton, J.A., Johnson, H.R., O'Brien, G.T., and Baumert, J.H. 1985, *Astrophys. J.*, **290**, 276.

Ferlet, R., and Gillet, D. 1984, *Astron. Astrophys.*, **133**, L1.

Fox, M.W., and Wood, P.R. 1982, *Astrophys. J.*, **259**, 198.

Fox, M.W., and Wood, P.R. 1985, in preparation.

Fox, M.W., Wood, P.R., and Dopita, M.A. 1984, *Astrophys. J..*, **286**, 337.

Furenlid, I. 1984, *Astron. Astrophys.*, **140**, 49.

Giampapa, M.S. 1984, *Astrophys. J.*, **277**, 235.

Gillet, D., and Lafon, J.P.J. 1983, *Astron. Astrophys.*, **128**, 53.

Gillet, D., and Lafon, J.P.J. 1984, *Astron. Astrophys.*, **139**, 401.

Gillet, D., Maurice, E., and Baade, D. 1983, *Astron. Astrophys.*, **128**, 384.

Gilra, D.P. 1976, Mém. Soc. Roy. Sci. Liège, **9**, 77.

Goebel, J.H., and Johnson, H.R. 1984, *Astrophys. J. (Letters)*, **284**, L39.

Goldberg, L. 1979, *Quart. J. Roy. Astr. Soc.*, **20**, 361.

Gómez Balboa, A., and de la Reza, R. 1985, in preparation.

Goorvitch, D., Goebel, J.H., and Augason, G.C. 1980, *Astrophys. J.*, **240**, 588.

Gorbatskii, V.G. 1961, *Soviet Astronomy.*, **5**, 192.

Hagen, W., Stencel, R.E., and Dickinson, D.F. 1983, *Astrophys. J.*, **274**, 286.

Haisch, B.M., Linsky, J.L., and Basri, G.S. 1980, *Astrophys. J..*, **235**, 519.

Hall, D.N.B., and Ridgway, S.T. 1977, in *Proc. IAU Collog. 21, Les Spectres des Molecules Simples au Laboratoire et en Astrophysique* (Liège, Belgium: Univesité de Liège), p. 243.

Hartmann, L., and Avrett, E.H. 1983, *Astrophys. J.*, **284**, 238.

Hayes, M.A., and Nussbaumer, H. 1984, *Astron. Astrophys.*, **134**, 194.

Heasley, J.N., Ridgway, S.T., Carbon, D.F., Milkey, R.W., and Hall, D.N. 1978, *Astrophys. J.*, **219**, 970.

Hill, S.J., and Willson, L.A. 1979, *Astrophys. J.*, **229**, 1029.

Hinkle, K.H. 1983, *Pub. Astron. Soc. Pacific*, **95**, 550.

Hinkle, K.H., Hall, D.N.B., and Ridgway, S.T. 1982, *Astrophys. J.*, **252**, 697.

Hinkle, K.H., and Lambert, D.L. 1975, *Mon. Not. Roy. Astr. Soc.*, **170**, 447.

Hinkle, K.H., Scharlach, W.W.G., and Hall, D.N.B. 1984, *Astrophys. J. Supplement*, **56**, 1.

Holzer, T.E., Flå, T., and Leer, E. 1983, *Astrophys. J.*, **275**, 808.

Hubený, I., and Heinzel, P. 1984, *J. Quant. Spect. Rad. Transf.*, **32**, 159.

Jefferies, J.T. 1968, *Spectral Line Formation*, (Waltham: Blaisdell).

Jennings, M.C. 1973, *Astrophys. J.*, **185**, 197.

Jennings, M.C., and Dyck, H.M. 1972, *Astrophys. J.*, **177**, 427.

Johnson, H.R. 1973, *Astrophys. J.*, **180**, 81.

Johnson, H.R. 1982, *Astrophys. J.*, **260**, 254.

Johnson, H.R., Bernat, A.P., and Krupp, B. 1980, *Astrophys. J. Supplement*, **42**, 501.

Johnson, H.R., Goebel, J.H., Goorvitch, D., and Ridgway, S.T. 1983, *Astrophys. J. (Letters)*, **270**, L63.

Johnson, H.R., and O'Brien, G.T. 1983, *Astrophys. J.*, **265**, 952.

Joy, A.H. 1947, *Astrophys. J.*, **106**, 288.

Kalkofen, W. 1985, to appear in *Proc. Sacramento Peak Workshop, Chromospheric Diagnosis and Modeling*, ed. B. Lites.

Kamijo, F. 1963a, *Pub. Astron. Soc. Japan*, **14**, 271.

Kamijo, F. 1963b, *Pub. Astron. Soc. Japan*, **15**, 440.

Keeley, D.A. 1970, *Astrophys. J.***161**, 634.

Kneer, F. 1983, *Astron. Astrophys.*, **128**, 311.

Lambert, D. L., and Snell, R.L. 1975, *Mon. Not. Roy, Astr. Soc.*, **172**, 277.

Leung, K.C., and Stothers, S.R. 1977, *J. Brit. Astron. Assoc.*, **87**, 263.

Linsky, J.F. 1980, *Ann. Rev. Astron. Astrophys.*, **18**, 439.

Linsky, J.F. 1981, in *Physical Processes in Red Giants*, ed. I. Iben and A. Renzini (Dordrecht: Reidel), p. 247.

Linsky, J.F. 1984a, *Mass Loss from Red Giants*, (Los Angeles: Univ. California), preprint.

Linsky, J.F. 1984b, *Progress in Stellar Spectra Line Formation* (Trieste), ed. J.E. Beckman and L. Crivellari (Dordrecht: Reidel).

Lites, B., and Mihalas, D 1984, *Solar Physics*, **93**, 25.

Livi, S., and Bergmann, T. 1982, *Astron. J.*, **87**, 1783.

Luck, R.E. 1977, *Astrophys. J.*, **218**, 752.

Luck, R.E., and Lambert, D.L. 1982, *Astrophys. J.*, **256**, 189.

Maciel, W.J. 1976, *Astron. Astrophys.*, **48**, 27.

Maciel, W.J. 1977, *Astron. Astrophys.*, **57**, 273.

Merchant, A.E. 1967, *Astrophys. J.*, **147**, 587.

Merrill, P.W. 1945, *Astrophys. J.*, **102**, 347.

Mihalas, D. 1978, *Stellar Atmospheres*, 2d ed. (San Francisco: W.H. Freeman and Co.).

Moon, T.T., Coates, D.W., Innis, J.L., and Thompson, K. 1983, *Inf. Bull. Var. Stars*, p. 2394.

Mount, G.H., Ayres, T.R., and Linsky, J.L. 1975, *Astrophys. J.*, **200**, 383.

Mount, G.H., and Linsky, J.L. 1975, *Solar Phys.*, **41**, 17.

Muchmore, D., and Ulmschneider, P. 1985, *Astron. Astrophys.*,**142**, 393.

Musielak, Z., and Sikorski, J. 1981, *Acta Astronom.*, **31**, 493.

Newell, R.T., and Hjellming, R.M. 1982, *Astrophys. J., (Letters)*, **263**, L85.

O'Brien, G.T. 1980, Thesis, Univ. of Texas.

Ostlie, D.A., Cox, A.N., and Cahn, J.H. 1982, in *Pulsations in Classical and Cataclysmic Variable Stars*, ed. J.P. Cox and C.J. Hansen (Boulder: Joint Inst. for Laboratory Astrophys), reprint, p. 297.

Querci, F. 1972, Thesis, Université de Paris.

Querci, F., and Querci, M. 1975, *Astron. Astrophys.*, **39**, 113.

Querci, M., and Querci, F. 1985, *Astron. Astrophys.*, **147**, 121.

Querci, F., Querci, M., Wing, R.F., Cassatella, A., and Heck, A. 1982, *Astron. Astrophys.*, **111**, 120.

Ramsey, L.W. 1977, *Astrophys. J.*, **215**, 827.

Ramsey, L.W. 1981, *Astrophys. J.*, **245**, 984.

Richer, H.B. 1975, *Astrophys. J.*, **197**, 611.

Schmid-Burgk, J., Scholz, M., and Wehrse, R. 1981, *Mon. Not. Roy. Astr. Soc.*, **194**, 383.

Schmitz, F., and Ulmschneider, P. 1981, *Astron. Astrophys.*, **93**, 178.

Schwarzschild, M. 1975, *Astrophys. J.*, **195**, 137.

Slutz, S. 1976, *Astrophys. J.*, **210**, 750.

Smith, M.A. 1980, *Space Sci. Rev.*, **27**, 307.

Smith, M.A. 1983, *Astrophys. J.*, **265**, 325.

Steenbock, W., and Holweger, H. 1984, *Astron. Astrophys.*, **130**, 319.

Stencel, R.E. 1982a, *Second Cambridge Workshop on Cool Stars*, SAO Special Rep., **392**, 137.

Stencel, R.E. 1982b, in *IAU Symp. 102, Solar and Stellar Magnetic Fields: Origins and Coronal Effects*, ed. J.O. Stenflo (Dordrecht: Reidel).

Stencel, R.E., Linsky, J.L., Brown, A., Jordan, C., Carpenter, K.G., Wing, R.F., and Czyzak, S. 1981, *Mon. Not. Roy. Acad. Sci.*, **196**, 47.

Tielens, A.G.G.M. 1983, *Astrophys. J.*, **271**, 702.

Thomas, R.N. 1960, *Astrophys. J.*, **131**, 429.

Thompson, R.I. 1973, *Astrophys. J.*, **181**, 1039.

Tsuji, T. 1983, *Astron. Astrophys.*, **122**, 314.

Tuchman, Y., Sack, N., and Barkat, Z. 1978, *Astrophys. J.*, **219**, 183.

Ulmschneider, P. 1979, *Space Sci. Rev.*, **24**, 71.

Vaiana, G.S., et al. 1981, *Astrophys. J.*, **245**, 163.

Vernazza, J.E., Avrett, E.M., and Loeser, R. 1981, *Astrophys. J.* Supplement, **45**, 635.

Whitney, C.A., and Skalafuris, A.J. 1963, *Astrophys. J.*, **138**, 200.

Wilson, O.C. 1957, *Astrophys. J.*, **126**, 46.

Wilson, O.C. 1960, *Astrophys. J.*, **131**, 75.

Wilson, O.C. 1982, *Astrophys. J.*, **257**, 179.

Wilson, O.C., and Bappu, M.K.V. 1957, *Astrophys. J.*, **125**, 661.

Willson, L.A. 1976, *Astrophys. J.*, **205**, 172.

Willson, L.A. 1982, in *Pulsations in Classical and Cataclysmic Variable Stars*, ed. J.P. Cox and C.J. Hansen (Boulder: Joint Inst. Laboratory Astrophys.) reprint, p. 269.

Willson, L.A., and Hill, S.J. 1979, *Astrophys. J.*, **228**, 854.

Willson, L.A., and Pierce, J.N. 1982, in *Second Cambridge Workshop on Cool Stars*, ed. M.S. Giampapa and Golub, Smithsonian Astrophys. Obs. Special Report, **392**, p. 147.

Willson, L.A., Wallerstein, G., and Pilachowski, C.A. 1982, *Mon. Not. Roy. Acad. Sci.*, **198**, 483.

Winkler, K.-H.A., Norman, M.L., and Mihalas, D. 1984, *J. Quant. Spect. Rad. Transf.*, **31**, 473.

Wood, P.R. 1974, *Astrophys. J.*, **190**, 609.

Wood, P.R. 1975, *Mon. Not. Roy. Astr. Soc.*, **171**, 15.

Wood, P.R. 1979, *Astrophys. J.*, **227**, 220.

Wood, P.R. 1980, in *Physical Processes in Red Giants*, ed. I. Iben and A. Renzini (Dordrecht: Reidel) p. 205.

Wood, P.R. 1982, in *Pulsations in Classical and Cataclysmic Variable Stars*, ed. J.P. Cox and C.J. Hansen (Boulder: Joint Inst. Laboratory Astrophys.) reprint, p. 284.

Yamashita, I. 1972, *Ann. Tokyo Astr. Obs.*, **13**, 169.

Yamashita, I. 1975, *Ann. Tokyo Astr. Obs.*, **15**, 47.

Zarro, D.M. 1984, *Astrophys. J.*, **285**, 232.

Zeldovich, Y.B., and Raizer, Y.P. 1966, *Physics of Shock Waves and High-Temperature Phenomena* (New York: New York Academic Press).

Zirin, H. 1982, *Astrophys. J.*, **260**, 655.